

# FERROELECTRICITY IN POTASSIUM DIHYDROGEN PHOSPHATE

David M. Finlayson

A Thesis Submitted for the Degree of PhD  
at the  
University of St Andrews



1951

Full metadata for this item is available in  
St Andrews Research Repository  
at:  
<http://research-repository.st-andrews.ac.uk/>

Please use this identifier to cite or link to this item:  
<http://hdl.handle.net/10023/14635>

This item is protected by original copyright

FERROELECTRICITY  
in  
POTASSIUM DIHYDROGEN PHOSPHATE  
being a thesis presented by  
David M. Finlayson B.Sc.  
to the University of St. Andrews  
in application for the degree of PH.D.



ProQuest Number: 10167162

All rights reserved

INFORMATION TO ALL USERS

The quality of this reproduction is dependent upon the quality of the copy submitted.

In the unlikely event that the author did not send a complete manuscript and there are missing pages, these will be noted. Also, if material had to be removed, a note will indicate the deletion.



ProQuest 10167162

Published by ProQuest LLC (2017). Copyright of the Dissertation is held by the Author.

All rights reserved.

This work is protected against unauthorized copying under Title 17, United States Code  
Microform Edition © ProQuest LLC.

ProQuest LLC.  
789 East Eisenhower Parkway  
P.O. Box 1346  
Ann Arbor, MI 48106 – 1346

Ms

1,122



### DECLARATION.

I hereby declare that the following Thesis is based on the results of experiments carried out by me, that the Thesis is my own composition, and that it has not previously been presented for a Higher Degree.

The Research has been carried out in the Physical Laboratory of the United College of the University of St. Andrews under the direction of Professor J.F.Allen, F.R.S.

CERTIFICATE.

I certify that David M. Finlayson, B.Sc. has spent nine terms in Research Work under my direction, that he has fulfilled the Conditions of Ordinance No.16 (St. Andrews) and is qualified to submit the accompanying Thesis in application for the Degree of Doctor of Philosophy.

Director of Research.

### CAREER.

I matriculated in the University of St. Andrews in October 1937 and graduated B.Sc. (Ordinary, Mathematics and Physics) in June 1940. After five and a half years army service, I returned to St. Andrews in 1946 and obtained First Class Honours in Physics in June 1947. In October 1947, I commenced the research on Ferroelectrics which is now being submitted as a Ph.D. Thesis. I was awarded a Tyndall-Bruce Scholarship in 1937, a Berry Research Scholarship in 1947 and a Carnegie Research Fellowship in October 1950.

I should like to express my sincere thanks to Professor J.F.Allen, F.R.S. for the keen interest he has shown throughout the course of these investigations, to Mr H.M.Barkla, M.A. for his suggestions and helpful criticism, to the University of St. Andrews for financial assistance, and to Mr J. Gerrard for his help in the preparation of the diagrams.

### SUMMARY.

A brief survey of ferroelectrics and a statement of the purpose of the present research are given. The necessary piezoelectric equations are developed and, using Mueller's theory of Rochelle salt as a basis, a phenomenological theory for potassium dihydrogen phosphate is worked out. Measurements of the electro-mechanical constants in the Curie region are reported. The experimental results are discussed in terms of the phenomenological theory and compared with a theory proposed by W.P. Mason. Since neither offers an adequate explanation of the results, the possibility of domain wall movement is considered. Crystal growth and experimental techniques are also discussed.

# C O N T E N T S.

	<u>Page</u>
1. <u>INTRODUCTION.</u>	1
1.1. SURVEY OF FERROELECTRICS.	1
1.2. SUMMARY OF THE PRESENT STATE OF KNOWLEDGE OF $\text{KH}_2\text{PO}_4$ .	8
1.3. THE PRESENT PROBLEM.	12
<hr/>	
2. <u>THEORY.</u>	15
2.1. PIEZOELECTRIC THEORY.	15
2.2. FERROELECTRIC THEORY.	19
2.3. TO FIND A RELATION FOR THE COERCIVE FIELD FROM MASON'S THEORY.	24
<hr/>	
3. <u>METHODS OF MEASUREMENT.</u>	26
3.1. MEASUREMENTS OF THE ELASTIC CONSTANTS.	26
3.2. MEASUREMENTS OF THE DIELECTRIC CONSTANTS.	30
3.3. CALCULATION OF THE PIEZOELECTRIC CONSTANTS.	31
3.4. MEASUREMENT OF TEMPERATURE.	32
3.5. ERRORS.	32
<hr/>	
4. <u>DISCUSSION OF THE RESULTS.</u>	38
4.1. ELASTIC CONSTANTS.	38
4.2. PIEZOELECTRIC CONSTANTS.	44
4.3. DIELECTRIC CONSTANTS.	49
4.4. CALCULATIONS FROM THE PHENOMENOLOGICAL THEORY.	53

	<u>Page</u>
4.5. CALCULATIONS FROM MASON'S THEORY.	55
4.6. THE FREE AND CLAMPED DIELECTRIC CONSTANTS $K_x$ .	58
4.7. GENERAL DISCUSSION.	69
4.8. POSSIBLE FUTURE RESEARCH.	68
<hr/>	
5. <u>CRYSTAL GROWTH</u> .	70
5.1. THE SEARCH FOR A SUITABLE TECHNIQUE.	79
5.2. SUMMARY OF CRYSTAL GROWING TECHNIQUE.	78
5.3. THEORIES OF CRYSTAL GROWTH.	80
5.4. OBSERVATIONS MADE DURING THE GROWTH OF. KDP CRYSTALS.	82
5.5. DISCUSSION.	83
<hr/>	
6. <u>EXPERIMENTAL METHODS</u> .	89
6.1. TEMPERATURE CONTROL OF THE CRYSTAL TANK.	89
6.2. CRYSTAL CUTTING AND GRINDING.	90
6.3. ELECTRODES.	91
6.4. CRYSTAL HOLDER.	92
6.5. GAS CRYOSTAT.	94
6.6. THERMOSTAT.	96
6.7. TEMPERATURE MEASUREMENT.	100
6.8. THE CLICK CIRCUIT.	100
6.9. MEASUREMENT OF THE RESONANT FREQUENCY.	102
6.10. MEASUREMENT OF THE DIELECTRIC CONSTANT AT LOW FREQUENCY.	104
6.11. MEASUREMENT OF THE DIELECTRIC CONSTANT AT HIGH FREQUENCY.	106
<hr/>	
REFERENCES	108
SYMBOLS	110
<hr/>	

1.1. SURVEY OF FERROELECTRICS.1.1.1. Experimental.

Although spontaneous magnetic polarisation had long been familiar, attention was not drawn to the electrical analogy of ferromagnetism until 1921, when Valasek (1) published the first of a series of papers on the peculiar properties of Rochelle salt ( $\text{NaKC}_4\text{H}_4\text{O}_6 \cdot 4\text{H}_2\text{O}$ ).

Just as in the ferromagnetic case, there is a certain temperature, called the Curie temperature, at which a spontaneous polarisation appears. The dielectric constant  $k'$  for the free crystal is characterised by a large maximum at or near the Curie point. Below this temperature, ( $24^\circ\text{C.}$ ), the relation between field and polarisation is not linear and the crystal shows dielectric hysteresis. In contrast to the ferromagnetic case, Rochelle salt possesses a lower Curie point, ( $-18^\circ\text{C.}$ ), below which the properties again become normal.

None of the substances isomorphous with Rochelle salt is ferroelectric but certain mixed crystals, obtained by replacing the K by  $\text{NH}_4$ , Rb or Tl, are ferroelectric in certain proportions.

Substitution of deuterium for hydrogen in Rochelle salt brings the Curie points closer together.

(1) References are given on page 108.



Rochelle salt has a complex structure which was not known until 1941. Meanwhile, a large number of papers dealing with its elastic, piezoelectric, dielectric and ferroelectric properties had been published, but theories proposed to explain them were necessarily hindered by lack of knowledge of the structure.

Study of the second group of ferroelectrics, comprising the phosphate and arsenate of potassium together with certain isomorphs, was begun in 1935 by Busch and Scherrer (2). The structure of potassium dihydrogen phosphate,  $\text{KH}_2\text{PO}_4$  (the abbreviation KDP is often used), was already known and was much simpler than that of Rochelle salt. This made an adequate theory seem to be more easily within reach. KDP suffers from the disadvantage of having its Curie point at  $121^\circ\text{K}$ .

The third group was begun in 1943, when von Hippel (3) confirmed that barium titanate ceramics showed ferroelectric properties. Since then, a number of similar compounds has been added to this group. Barium titanate has a Curie point at  $120^\circ\text{C}$ . and is thus easily accessible at room temperature. It remains ferroelectric down to very low temperature with two further transitions at about  $0^\circ\text{C}$ . and  $-70^\circ\text{C}$ . Moreover, it has a simple, perovskite structure. Although early experiments were done on ceramics, single crystals have now been produced. On account of the simple structure and the accessibility of the ferroelectric temperature range, as well as the

possibility of technical applications, recent research has tended to concentrate on the titanate group. Meanwhile, several problems in the second group have remained unsolved. These are discussed further in 1.2 and 1.3.

#### 1.1.2. Theories.

The first attempt at a theory of Rochelle salt was made by Kurchatov in 1930. In this it was assumed that Rochelle salt contained rotatable dipoles, each having a moment of about 1 debye unit. Following the lines of Debye's dipolar theory, Kurchatov calculated that the dipole-dipole interaction was sufficient to account for spontaneous polarisation below a critical temperature. To account for the lower Curie point, he rather weakly postulates "reciprocal action", which leads to the formation of mutually neutralising chains at lower temperatures.

Fowler also developed a theory in terms of rotating dipoles along somewhat similar lines.

Both these theories had ignored the fact that piezoelectric reaction must play an important part in the behaviour of ferroelectrics.

Mueller was the first to develop a theory which took account of the piezoelectric properties. In his first paper (4) he used the concept of the internal field. Later, however, he abandoned this and, using his experimental findings, worked out a more strictly phenomenological theory (5). His experiments showed that, over

the whole temperature range, the piezoelectric stresses are proportional to the polarisation rather than to the field, and that only the dielectric properties of the rigidly clamped crystal remain anomalous at the Curie point when the energy is expressed in terms of polarisation. He then introduced a term in  $P^3$  in the expression for  $E$  to account for the non-linearity between  $E$  and  $P$  and was able to predict the existence of a spontaneous polarisation between the Curie points. A more complete account of his theory will be given in 2.2.

The publication of the work of Beevers and Hughes (6) on the structure of Rochelle salt, coupled with the discovery of ferroelectricity in KDP, turned attention to the properties of the hydrogen bond O-H-O in both these substances.

In 1947, W.P.Mason developed a theory of Rochelle salt in terms of the hydrogen bonds in the crystal.(7). The bond in question is between a water molecule and an oxygen ion and is, therefore, likely to be asymmetric. By calculating the probability of a hydrogen nucleus in one potential well jumping into another of different depth, he obtains expressions for the polarisation, dielectric constant and coercive field which seem to agree fairly well with experiment.

This theory is simpler in the case of the symmetric bond which occurs in KDP. Mason's findings for the polarisation, dielectric constant and coercive field are

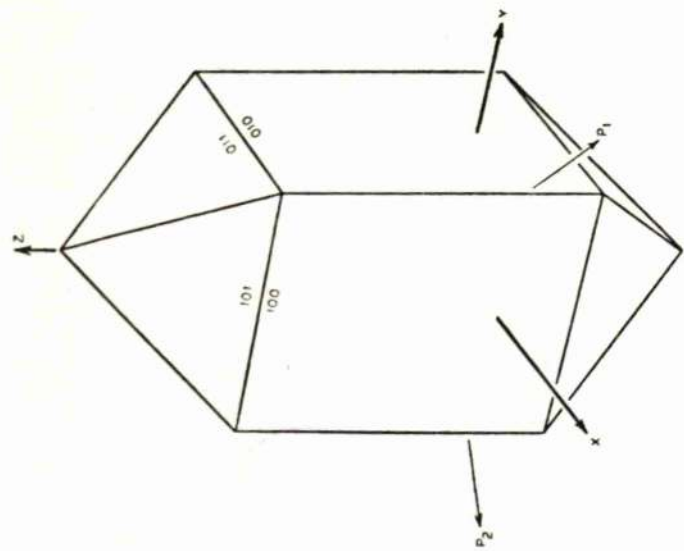
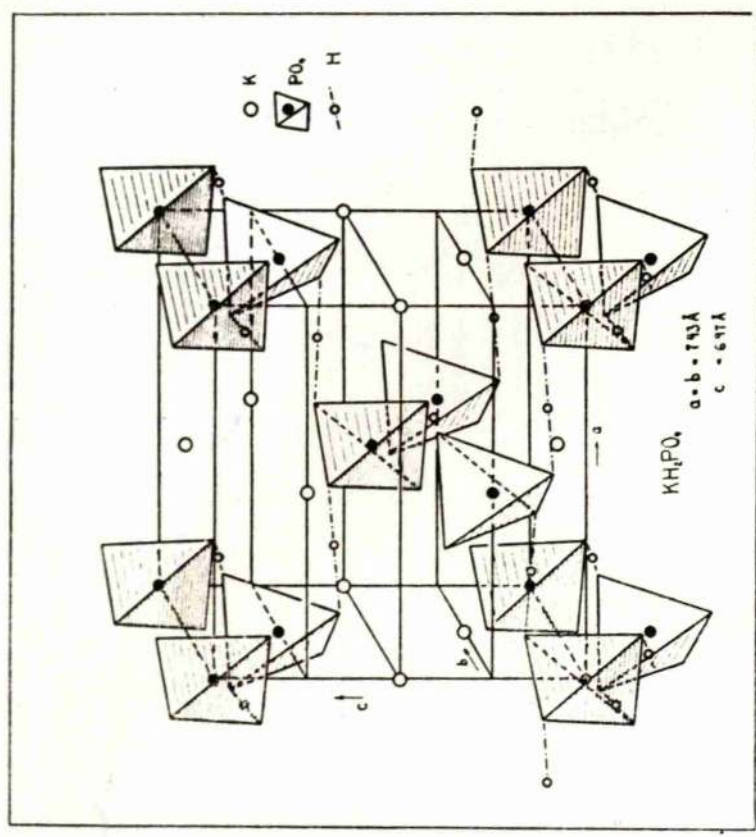


FIG. 1. Growth habit for ADP and KDP.



Elementary cell of crystal lattice of H<sub>2</sub>KPO<sub>4</sub>.

From W.P.Mason.



discussed in 4. He has developed a similar theory for the somewhat different structure of the titanates.

A theory of the ferroelectricity of KDP has been developed by Slater (8), using statistical methods. The background to his theory is as follows:-

From the structure of KDP, as given by West (9) (diagram on page 5), it is believed that the potassium atoms do not play an important part but serve to hold the crystal together. The phosphate group and hydrogen ions are responsible for the dielectric behaviour. A phosphate group consists of a phosphorous atom tetrahedrally surrounded by four oxygen atoms. Each phosphate group is in turn tetrahedrally surrounded by four other phosphate groups. The position of the hydrogens is not actually shown by X-rays but symmetry suggests that one hydrogen lies on the line joining the nearest oxygens of adjacent phosphate groups. The hydrogens are probably not in the middle of the O-H-O bond but lie nearer one or other of the oxygens. The lengths of the hydrogen bonds lie at a small angle to the *a* and *b* axes. It is supposed that the energy required to form the ions ( $\text{HPO}_4$ ) or ( $\text{H}_3\text{PO}_4$ ) is sufficiently high to make them very unlikely to occur so that each phosphate group will have only two hydrogens near it, the other two hydrogens being attached to neighbouring groups. There are six possible arrangements of these hydrogens:- 1) Two hydrogens up (along *c* axis); 2) Two hydrogens down; 3,4,5 and 6) One up and one

down. Each of these arrangements makes the  $(\text{H}_2\text{PO}_4)$  group an electric dipole which points 1) along the positive c axis; 2) along the negative c axis; 3,4,5 and 6) in a plane perpendicular to c. Since the c axis is a preferred direction, the dipoles oriented along the + or -c axis will have an energy different from those perpendicular to c. In fact, they will have a lower energy. Hence, there is a tendency towards spontaneous polarisation at low temperatures, not because of dipole-dipole interaction, but because each individual dipole has a lower energy when oriented along the c axis.

By a simple statistical theory, Slater calculates the number of arrangements having a given energy, computes the partition function and, from this, obtains the Helmholtz free energy and the entropy. His calculations suggest a first order change at the Curie point with a latent heat. A more rigid treatment yields essentially the same results and from this he obtains a value for the dielectric constant above the Curie point which shows reasonable agreement with experiment. His change of entropy at the Curie point is lower than the experimental value. To account for the observed transition, he suggests that, in a single domain crystal, a sharp transition occurs. In a multi-domain crystal, however, neighbouring domains polarised in opposite directions will, through the piezoelectric effect, shear in opposite directions and exert a pressure on each other, which will

lower the Curie point. Different pressures will exist throughout the crystal so that Curie points of domains will be lowered by varying amounts, thus spreading the transition over several degrees.

Slater seems to consider the polarisation as being caused by the motion of the hydrogens along the bond. It has been pointed out by De Quervain (10) that the hydrogens, by themselves, cannot account for the polarisation. De Quervain suggests that a distortion of the phosphate group accompanies the motion of the hydrogen atoms and the nett movement of charge is large enough to account for the observed polarisation.

A phenomenological theory of barium titanate has been worked out by Devonshire (11) on the lines of Mueller's theory but considering terms up to  $P^6$ . This gives qualitative agreement with experiment. Devonshire has also given an atomic theory of barium titanate which has recently been amplified by Slater (12).

#### 1.2. SUMMARY OF PRESENT STATE OF KNOWLEDGE OF $\text{KH}_2\text{PO}_4$ .

The ferroelectric properties of potassium dihydrogen phosphate were first discussed in a paper by Busch and Scherrer in 1935 (2). In 1938, Busch (13) published his main work on the subject, showing the temperature dependence of the dielectric constants along both axes.

Along the ferroelectric axis the dielectric constant rose from about 20 at room temperature to a value greater than

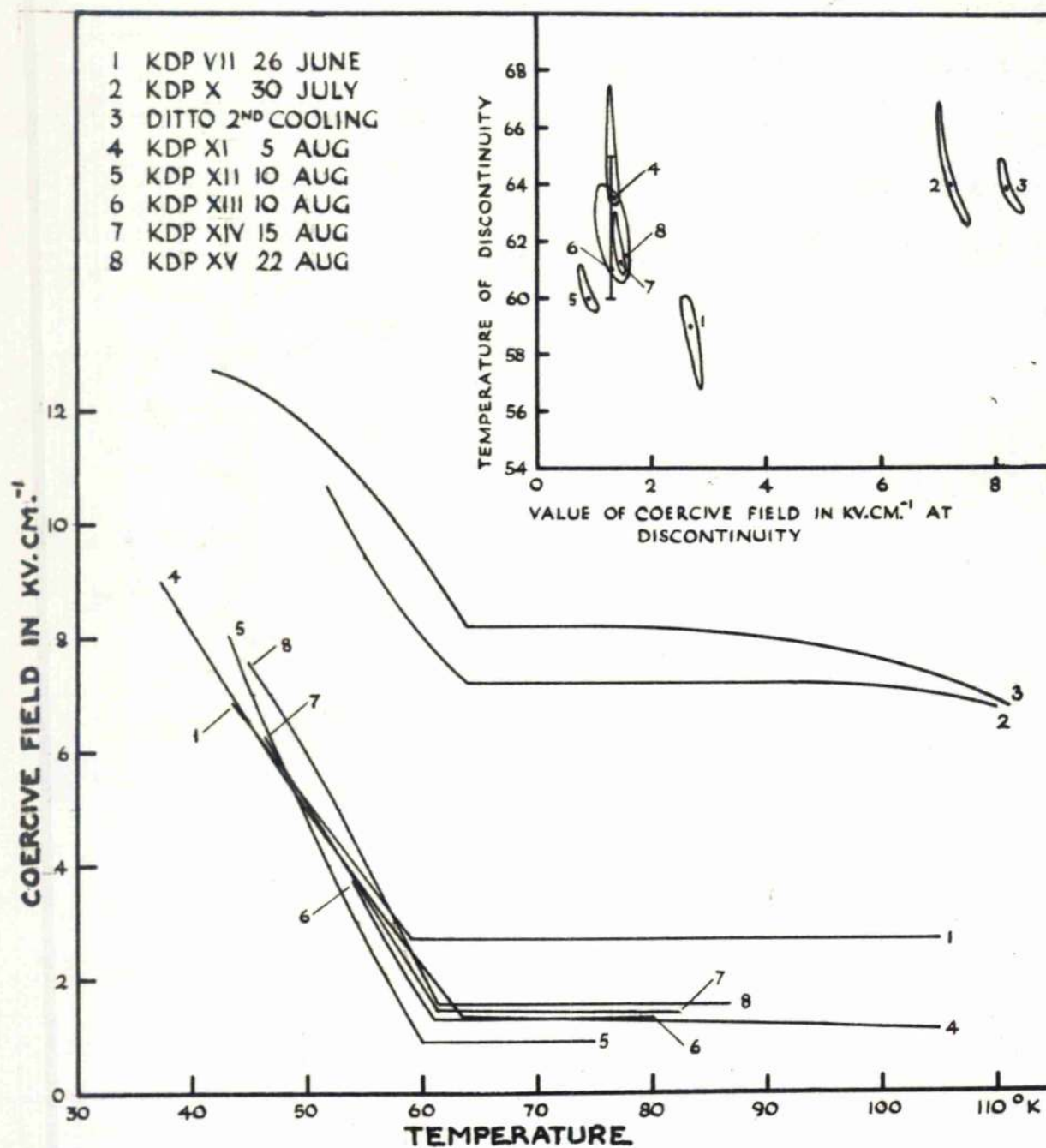
$10^4$  at the Curie point. The dielectric constant perpendicular to the ferroelectric axis, although not showing this extreme anomaly, had the high value of about 50 at room temperature, rising slightly to a maximum at the Curie point and then falling sharply. This behaviour contrasts with that of Rochelle salt, where the dielectric constants along the non-ferroelectric axes have normal values of about 9 with no anomaly at the Curie point. Busch was unable to reach temperatures below that of liquid air but his curve for  $k_z$  below the Curie point is interesting in that it tends to flatten out at about  $90^\circ\text{K}$  at a very high value.

An attempt was made in 1939 by Ganz in the Mond Laboratory to reach lower temperatures. The results were published in a joint paper with Busch (14). In this series of measurements they dealt with a complex dielectric constant. Although the measurements by Busch in 1938 were made at about 200 volts/cm. field strength, in their later work a field strength of about 2400 volts/cm. was used. This gave a somewhat lower value of  $k_z$  which was maintained down to a temperature of about  $80^\circ\text{K}$ , after which it fell rapidly. A series of hysteresis loops, obtained by applying an alternating field of 3000 volts/cm., was also shown down to  $58^\circ\text{K}$ . At this temperature, the hysteresis loops vanished. This was erroneously identified by some of the Swiss workers as a



lower Curie point. However, from Ganz's photographs, it is evident that the loops just above this temperature were not saturated and the vanishing of the loops was due, not to the disappearance of the spontaneous polarisation, but rather to an increase in the coercive field so that the field applied was no longer sufficient to reverse the domains. Moreover, subsequent work has shown that the coercive field down to about  $60^{\circ}\text{K}$  is in the region of 2000 volts/cm. while, below this temperature, the coercive field rises sharply. But the field used to measure the dielectric constant was 2400 volts, which is of the order of the coercive field above  $60^{\circ}\text{K}$  and is only a small fraction of it at, say,  $40^{\circ}\text{K}$ . Hence the measurements of  $k_z'$  given by Busch and Ganz can by no stretch of the imagination be called initial constants nor do they correspond to the overall dielectric constant over the complete range measured by them.

Several years were to elapse before the "lower Curie point" problem was finally settled. Meanwhile, indirect evidence against it accumulated. Specific heat measurements, while showing the expected anomaly at the Curie point, showed no trace of a further anomaly at the point where the hysteresis loops vanished. The electro-optical work of Zwicker and Scherrer (15) on the equivalent range of  $\text{KD}_2\text{PO}_4$  showed no sign of a lower Curie point, but an increase in the coercive field was observed.



From H.M.Barkla.

The question was tackled directly by Barkla (16) in 1946. He used a very large condenser to maintain a constant potential difference across a KDP crystal while its temperature was lowered. This showed conclusively that the spontaneous polarisation persisted down to at least  $20^{\circ}\text{K}$ . Barkla (unpublished) also showed that a sharp change occurred in the coercive field at about  $60^{\circ}\text{K}$ . The coercive field rose steeply from the Curie point to a value of about 2000 volts/cm. and thereafter remained approximately constant down to  $60^{\circ}\text{K}$ , below which it again rose steeply (page 11). The temperature of the discontinuity and the gradient at lower temperatures remained approximately constant for a number of crystals, although the actual level of the coercive field tended to rise after successive coolings.

In 1946, Mason (17) published a fairly complete account of the electro-mechanical behaviour of KDP above the Curie point.

### 1.3. THE PRESENT PROBLEM.

When this research was begun, measurements on KDP below the Curie point were very incomplete, presumably because of the difficult temperature range involved. No measurements of elastic or piezoelectric constants of any kind appear to have been attempted. The only measurements of the dielectric constants down to fairly low temperatures were those of Busch and Ganz and these

were taken in such a way as to be practically meaningless. The only reliable measurements appear to be the hysteresis loops of Ganz and Barkla and the coercive field-temperature relationship of the latter.

The present research was therefore undertaken to fill in as much of this gap as possible by extending the electro-mechanical measurements of Mason down to the temperature of liquid hydrogen. This work appeared all the more necessary in that, up to this time, theories of ferroelectricity had been dependent for experimental data on Rochelle salt. The behaviour of this substance is, however very greatly affected by the closeness of its two Curie points. Indeed, Mueller has suggested that if the crystal could be rigidly clamped it might not become ferroelectric at any temperature, since the piezoelectric reaction appears to play an essential part. Due also to the narrow ferroelectric region, there is no range of temperature over which the spontaneous polarisation and associated phenomena remain constant. To test theories built up for Rochelle salt, measurements were required on ferroelectrics which approximated more closely to the ferromagnetic analogy.

The sharp increase in the coercive field around  $60^{\circ}\text{K}$  presented a more specific problem. In the ferromagnetic case the coercive field was known to depend on the magnetostriction and Young's modulus. Although magnetostriction and piezoelectric deformation are by no

means strictly analogous, it nevertheless seemed plausible to expect in KDP some change in the elastic constants in the neighbourhood of  $60^{\circ}\text{K}$  denoting some change in the crystal structure.

Measurements of the elastic behaviour of the crystal below the Curie point were therefore planned.

To obtain bars suitable for making dynamic measurements, crystals having dimensions of at least 2 cms. in all directions were required. Preliminary experiments on crystal growth were begun and, at the same time, attempts were made to find a source of KDP in this country. After exhaustive enquiries, it was concluded that sufficiently large crystals were unobtainable. A portion of a crystal grown in Zürich was obtained via the Mond Laboratory in Cambridge and, ultimately, a few specimens of a Z45 cut were obtained from the Brush Crystal Coy. of U.S.A. By this time, however, crystal growing technique had been acquired and satisfactory home-grown crystals were ready.



## 2.

THEORY2.1. PIEZOELECTRIC THEORY

In the following section the notation adopted is that of Cady (18) while the methods and equations are mainly to be found in Cady and Mason (19).

2.1.1. Basic Equations

Using only the electro-mechanical terms, the free energy of a crystal under electrical and mechanical stress may be written as follows:-

$$\mathcal{F} = \frac{1}{2} \sum_h \sum_i c_{hi} x_h x_i + \frac{1}{2} \sum_h \sum_m \eta''_{hm} E_h E_m + \sum_m \sum_h e_{mh} E_m x_h \quad \text{--- (1a)}$$

$$\mathcal{J} = \frac{1}{2} \sum_h \sum_i s_{hi} X_h X_i + \frac{1}{2} \sum_h \sum_m \eta'_{hm} E_h E_m - \sum_m \sum_h d_{mh} E_m X_h \quad \text{--- (1b)}$$

where  $x$  = strain     $X$  = stress     $E$  = field strength

$c^E, s^E$  = elastic stiffness and compliance at constant field,

$\eta'', \eta'$  = electric susceptibility at constant strain and stress,

$d, e$  = the piezoelectric coefficients.

Differentiating eqns. (1a), (1b) with respect to strain and stress and keeping the field constant, we get:-

$$\frac{\partial \mathcal{F}}{\partial x_h} = \sum_i c_{hi} x_i = -X_h \quad \text{--- (2a)}$$

$$\frac{\partial \mathcal{J}}{\partial X_h} = \sum_i s_{hi} X_i = -x_h \quad \text{--- (2b)}$$

Differentiating eqn. (1a) with respect to strain and

field we get:-  $\frac{\partial \mathcal{F}}{\partial x_h} = \sum_i c_{hi}^E x_i + \sum_m e_{mh} E_m = -X_h \quad \text{--- (2c)}$

$$\frac{\partial \mathcal{F}}{\partial E_m} = \sum_h \eta''_{hm} E_h + \sum_h e_{mh} x_h = P_m \quad \text{--- (2d)}$$

where P is the polarisation.

Differentiating eqn. (1b) with respect to stress and field we get:-

$$\frac{\partial \mathcal{J}}{\partial X_k} = \sum_i^6 s_{ki}^E X_i - \sum_m^3 d_{mk} E_m = -\alpha_k \quad \text{--- (2e)}$$

$$\frac{\partial \mathcal{J}}{\partial E_m} = \sum_k^3 \eta'_{km} E_k - \sum_h^6 d_{mh} X_h = P_m \quad \text{--- (2f)}$$

For the symmetry of  $\text{KH}_2\text{PO}_4$  (tetragonal scalenohedral)

eqns. (2) reduce to :-

$$\begin{aligned} -X_x &= c_{11} \alpha_x + c_{12} y_y + c_{13} z_z & -\alpha_x &= s_{11} X_x + s_{12} Y_y + s_{13} z_z \\ -Y_y &= c_{12} \alpha_x + c_{11} y_y + c_{13} z_z & -y_y &= s_{12} X_x + s_{11} Y_y + s_{13} z_z \\ -Z_z &= c_{12} \alpha_x + c_{13} y_y + c_{33} z_z & -z_z &= s_{12} X_x + s_{13} Y_y + s_{33} z_z \end{aligned} \quad \text{--- (3a) --- (3b)}$$

$$\begin{aligned} -Y_z &= c_{44}^E y_z + e_{14} E_x & P_x &= \eta_x'' E_x + e_{14} y_z \\ -Z_x &= c_{44}^E z_x + e_{14} E_y & P_y &= \eta_x'' E_y + e_{14} z_x \\ -X_y &= c_{66}^E x_y + e_{36} E_z & P_z &= \eta_z'' E_z + e_{36} x_y \end{aligned} \quad \text{--- (3c) --- (3d)}$$

$$\begin{aligned} -y_z &= s_{44}^E Y_z - d_{14} E_x & P_x &= \eta_x' E_x - d_{14} Y_z \\ -z_x &= s_{44}^E z_x - d_{14} E_y & P_y &= \eta_x' E_y - d_{14} z_x \\ -x_y &= s_{66}^E X_y - d_{36} E_z & P_z &= \eta_z' E_z - d_{36} X_y \end{aligned} \quad \text{--- (3e) --- (3f)}$$

From eqns. (3) we then have the following constants:-

Elastic.  $c_{11}, c_{12}, c_{13}, c_{33}, c_{44}^E, c_{66}^E$ .

$s_{11}, s_{12}, s_{13}, s_{33}, s_{44}^E, s_{66}^E$ .

Dielectric.  $\eta'_x, \eta'_z$  -free  $X=0$ .  $\eta = 1/\chi = \frac{K-1}{4\pi}$   
 $\eta''_x, \eta''_z$  -clamped  $x=0$ .  $\eta'' = \eta' - de$ . — (4a)

Piezoelectric.  $d_{14}, d_{36}$ .  
 $e_{14}, e_{36}$ .  $e_{36} = \frac{d_{36}}{S_{66}^E} = d_{36} c_{66}^E$  — (4b)

These equations are in the form used by Voigt with the energy equations (1) written in terms of the field  $E$ .

It is, however, possible to rewrite eqns. (1) in terms of the polarisation  $P$  and the constants are then derived according to the "Polarisation" theory.

In an ordinary piezoelectric, both forms will give an adequate representation but in ferroelectrics, where the relation between  $E$  and  $P$  is not linear, considerable differences should emerge. From the work on Rochelle salt and KDP above the Curie point, it appears that the polarisation theory is the more satisfactory.

In terms of polarisation, eqns. (1) become:-

$$\mathcal{F} = \frac{1}{2} \sum_R \sum_i^6 c_{Ri}^P x_R x_i + \frac{1}{2} \sum_R \sum_m^3 \chi''_{Rm} P_R P_m + \sum_m \sum_R^6 a_{mR} P_m x_R \quad (5a)$$

$$\mathcal{F} = \frac{1}{2} \sum_R \sum_i^6 s_{Ri}^P X_R X_i + \frac{1}{2} \sum_R \sum_m^3 \chi'_{Rm} P_R P_m - \sum_m \sum_R^6 b_{mR} P_m X_R \quad (5b)$$

From these we get the additional constants:-

Elastic  $c_{44}^P, c_{66}^P, s_{44}^P, s_{66}^P$

Piezoelectric  $a_{14}, a_{36}$ .

$b_{14}, b_{36}$ .  $a_{36} = \frac{b_{36}}{s_{66}^P} = b_{36} c_{66}^P$  — (6)

The following relations connect the Voigt and Polarisation



constants:-

$$c_{44}^P = c_{44}^E + e_{14} a_{14} - (7a) \quad s_{44}^P = s_{44}^E - d_{14} b_{14} - (7b)$$

$$c_{66}^P = c_{66}^E + e_{36} a_{36} - (7c) \quad s_{66}^P = s_{66}^E - d_{36} b_{36} - (7d)$$

$$\chi_{x'}'' = \chi_{x'}' + b_{14} a_{14} - (7e) \quad \chi_z'' = \chi_z' + a_{36} b_{36} - (7f)$$

$$a_{14} = \frac{4\pi e_{14}}{K_{x'}''} - (7g) \quad a_{36} = \frac{4\pi e_{36}}{K_z''} - (7h)$$

$$b_{14} = \frac{4\pi d_{14}}{K_{x'}'} - (7i) \quad b_{36} = \frac{4\pi d_{36}}{K_z'} - (7j)$$

### 2.1.2. Equations for rotated axes.

The general equations are given by Cady p.70.ref.(18).

If the direction cosines  $\alpha, \beta, \gamma$  are given

by matrix

where XYZ are the crystal axes and X'Y'Z' the rotated axes, then for KDP the general equations reduce to the following:-

	X'	Y'	Z'
X	$\alpha_1$	$\beta_1$	$\gamma_1$
Y	$\alpha_2$	$\beta_2$	$\gamma_2$
Z	$\alpha_3$	$\beta_3$	$\gamma_3$

$$s_{11}' = \alpha_1^4 s_{11} + \alpha_2^4 s_{11} + \alpha_3^4 s_{33} + \alpha_2^2 \alpha_3^2 (2s_{13} + s_{44}) + \alpha_3^2 \alpha_1^2 (2s_{13} + s_{44}) + \alpha_1^2 \alpha_2^2 (2s_{12} + s_{66}) - (8a)$$

$$s_{44}' = 4\beta_1^2 \gamma_1^2 s_{11} + 4\beta_2^2 \gamma_2^2 s_{11} + 4\beta_3^2 \gamma_3^2 s_{33} + 8\beta_2 \gamma_2 \beta_3 \gamma_3 s_{13} + 8\beta_3 \gamma_3 \beta_1 \gamma_1 s_{13} + 8\beta_1 \gamma_1 \beta_2 \gamma_2 s_{12} - (8b) + (\beta_2 \gamma_3 + \beta_3 \gamma_2)^2 s_{44} + (\beta_3 \gamma_1 + \beta_1 \gamma_3)^2 s_{44} + (\beta_1 \gamma_2 + \beta_2 \gamma_1)^2 s_{66}$$

$$s_{66}' = 4\alpha_1^2 \beta_1^2 s_{11} + 4\alpha_2^2 \beta_2^2 s_{11} + 4\alpha_3^2 \beta_3^2 s_{33} + 8\alpha_2 \beta_2 \alpha_3 \beta_3 s_{13} + 8\alpha_3 \beta_3 \alpha_1 \beta_1 s_{13} + 8\alpha_1 \beta_1 \alpha_2 \beta_2 s_{12} - (8c) + (\alpha_2 \beta_3 + \alpha_3 \beta_2)^2 s_{44} + (\alpha_3 \beta_1 + \alpha_1 \beta_3)^2 s_{44} + (\alpha_1 \beta_2 + \alpha_2 \beta_1)^2 s_{66}$$

For a Z cut (8a) gives :-

$$S_{11}' = S_{11}(\sin^4 \varphi + \cos^4 \varphi) + (2S_{12} + S_{66})\sin^2 \varphi \cos^2 \varphi. \quad (9a)$$

where  $\varphi$  is the rotation about the Z axis from the X direction.

For an X cut (8a) reduces to :-

$$S_{11}' = S_{11} \cos^4 \theta + (2S_{13} + S_{44})\sin^2 \theta \cos^2 \theta + S_{33} \sin^4 \theta \quad (9b)$$

where  $\theta$  is the rotation about the X axis measured from Y

For a Z cut (8c) gives:-

$$S_{66}' = 2\sin^2 2\varphi (S_{11} - S_{12}) + \cos^2 2\varphi \cdot S_{66} \quad (9c)$$

where  $\varphi$  is the rotation about the Z axis from X

For an X cut (8b) gives:-

$$S_{44}' = \sin^2 2\theta (S_{11} + S_{33} - 2S_{13}) + \cos^2 2\theta S_{44} \quad (9d)$$

## 2.2. FERROELECTRIC THEORY.

An account will now be given of the interaction theory of ferroelectricity developed by H. Mueller as it is presented by Cady. The theory will be adapted somewhat to suit KDP and some of its conclusions tested by the measurements observed.

The theory is based on three main postulates:-

1. The relation between field strength E and polarisation P is not linear. A term in  $P^3$  is introduced in the expression for E. This appears in the energy equation as the term  $\frac{1}{4}BP^4$  where B is a constant.
2. The piezoelectric stress is proportional to P and not to E.

3. The dielectric properties of the clamped crystal are chiefly responsible for the ferroelectric behaviour.

KDP is tetragonal above the Curie point, but below the Curie point the lattice is distorted slightly and the crystal symmetry becomes orthorhombic.

In order to give a unified presentation it will be assumed that KDP is tetragonal at all temperatures so that a stress system must be assumed below the Curie point to bring the distorted crystal back to the tetragonal formation.

For the tetragonally clamped crystal we introduce  $\chi_1$  for the inverse dielectric susceptibility. Later, it will be necessary to discuss the clamping of the crystal in the deformed state and for this  $\chi'_s$  and  $\chi''_s$  will be used.

#### 2.2.1. Basic Equations.

For the energy equation (5) we write:-

$$\mathcal{F} = \frac{1}{2} c_{66}^P (x_y - x_y^0)^2 + \frac{1}{2} \chi_1 P_E^2 + \frac{1}{4} B P_E^4 + a_{36} P_E x_y \quad \text{--- (10a)}$$

$$\mathcal{J} = \frac{1}{2} s_{66}^P \chi_y^2 + \frac{1}{2} \chi'_1 P^2 + \frac{1}{4} B P^4 - b_{36} P \chi_y \quad \text{--- (10b)}$$

In a) the polarisation  $P_0$  is neutralised by the strain  $x_y^0$  so  $P_0$  does not appear in the equation.

In b) when  $\chi_y = 0$  the energy must include  $P_0$  so  $P = P_0 + P_E$  is used in the equation.

Differentiating, we get:-

$$\frac{\partial \mathcal{F}}{\partial x_y} = c_{66}^P x_y - c_{66}^P x_y^0 + a_{36} P_E = -(\chi_y) \quad \text{--- (11a)}$$

$$\frac{\partial \mathcal{J}}{\partial P_E} = \chi_1 P_E + B P_E^3 + a_{36} x_y = (E)'' \quad \text{--- (11b)}$$

$$\frac{\partial J}{\partial X_y} = s_{66}^P X_y - b_{36} P = -x_y \quad \text{---(11c)}$$

$$\frac{\partial J}{\partial P_E} = \chi' P + B P^3 - b_{36} X_y = (E)' \quad \text{---(11d)}$$

$(X_y)$  is the body stress and equals the external stress added to that caused piezoelectrically by  $P$ .

$(E)''$  is the field that in a clamped crystal would produce the same polarisation as that given by  $P$  and  $X_y$ .

In c) if  $E=0=X_y$  then  $P = P_0$

$$\text{so } x_{y0} = b_{36} P_0$$

$$\text{also } -(X_y) = -X_y + 2a_{36} P_E.$$

(11a) becomes .

$$c_{66}^P x_y - c_{66}^P b_{36} P_0 + a_{36} P_E - 2a_{36} P_E = -X_y$$

$$\text{but } b_{36} = a_{36} s_{66}^P$$

$$\text{so } c_{66} x_y - a_{36} (P_0 + P_E) = -X_y. \quad \text{---(12a)}$$

Since  $P_E$  is the polarisation when  $x_y = 0$

$$E = \chi_1 P_E + B P_E^3$$

so

$$(E)'' = \chi_1 P_E + B P_E^3 + a_{36} x_y = E + a_{36} x_y = \chi_1 P_t + B P_t^3 \quad \text{---(12b)}$$

$$-x_y = s_{66} X_y - b_{36} P. \quad \text{---(12c)}$$

$$(E)' = \chi' P + B P^3 - b_{36} X_y = E - b_{36} X_y = \chi' P_t + B P_t^3 \quad \text{---(12d)}$$

$P_t$  is the sum of the contributions from  $x_y$  and  $P_E$

2.2.2. To find an expression for the free reciprocal susceptibility.

In (12c) let  $X_y = 0$

then  $x_y = b_{36} P$  where  $P$  is due to  $E$  alone.

Substituting in (12b)

$$E + a_{36} b_{36} P = \chi_1 P_t + B P_t^3.$$

but  $P$  is now the total polarisation  $P_t$

$$\text{so } E + a_{36} b_{36} P = \chi_1 P + B P^3$$

$$\therefore E = (\chi_1 - a_{36} b_{36})P + B P^3 \quad \text{---(13)}$$

$P$  is the polarisation due to  $E$  in the free crystal (since  $X_y = 0$ ) and so (13) must be equivalent to (12d).

$$\text{then } E = (\chi_1 - a_{36} b_{36})P + B P^3 = \chi' P + B P^3 \quad \text{---(14)}$$

$$\text{where } \chi' = \chi_1 - a_{36} b_{36}$$

$$\text{when } E = 0, \quad P_E = 0$$

$$\therefore B P_0^2 = -(\chi_1 - a_{36} b_{36}) = -\chi' \quad \text{---(15)}$$

This gives a real solution if  $\chi_1 < a_{36} b_{36}$

Hence the condition for ferroelectricity to occur is that the dielectric constant of the tetragonally clamped crystal should be less than the product  $a_{36} b_{36}$ .

### 2.2.3. The Constant B.

An estimate of the value of the constant  $B$  can be obtained from measurements of the field dependence of the dielectric constant in the region just above the Curie point in the following manner:-

$$\text{eqn. (14) gives } E = \chi' P + B P^3$$

$$\therefore 1 = \frac{dP}{dE} (\chi' + 3B P^2)$$

$$\text{but } \frac{dP}{dE} = \eta \quad \text{and } \chi' = \frac{1}{\eta_0}$$

$$\text{so } \frac{1}{\eta_E} = \frac{1}{\eta_0} + 3B P^2$$

$$\therefore 3B P^2 = \frac{\eta_0 - \eta_E}{\eta_E \eta_0} = X = \frac{4\pi(K_0 - K_E)}{K_0 K_E}$$

so

$$P = \left( \frac{X}{3B} \right)^{\frac{1}{2}}$$

substituting in eqn. (14).

$$E = \chi' \left( \frac{X}{3B} \right)^{\frac{1}{2}} + B \left( \frac{X}{3B} \right)^{\frac{3}{2}}$$

$$\therefore \frac{E}{X^{\frac{1}{2}}} = \frac{\chi'}{(3B)^{\frac{1}{2}}} + \frac{X}{3(3B)^{\frac{1}{2}}} \quad \text{--- (16)}$$

$\chi'$  is a constant for any particular temperature, hence  $\frac{E}{X^{\frac{1}{2}}}$  plotted against  $X$  should yield a straight line from the gradient of which  $B$  can be calculated.

#### 2.2.4. To find an expression for the free reciprocal susceptibility below the Curie point.

In the previous section it was found that

$$B P_0^2 = -(\chi_1 - a_{36} b_{36}) = -\chi' \quad \text{--- (15)}$$

so, for a real value of  $P_0$ ,  $\chi'$  must be negative.

Hence  $\chi'$  cannot correspond to an observable quantity in the Curie region.

Going back to equation (14) we have:-

$$E = \chi' P + B P^3$$

where  $P = P_0 + P_E$ .

$$\therefore E = \chi' (P_0 + P_E) + B (P_0 + P_E)^3 \quad \text{--- (17)}$$

The value of the free initial susceptibility below the Curie point  $\eta_s'$  is obtained from this equation by differentiation,

$$\eta_s' = \left( \frac{\partial P}{\partial E} \right)_{P_E=0} = \text{the initial slope of the } E : P \text{ curve}$$

$$\therefore 1 = \chi' \frac{\partial (P_E + P_0)}{\partial E} + 3B (P_0 + P_E)^2 \frac{\partial (P_E + P_0)}{\partial E}$$

then

$$\frac{\partial (P_E + P_0)}{\partial E} = \frac{1}{\chi' + 3B(P_0 + P_E)^2}$$

$$\text{so } \eta'_s = \left[ \frac{\partial (P_0 + P_E)}{\partial E} \right]_{P_E=0} = \frac{1}{\chi' + 3BP_0^2}$$

$$\therefore \chi'_s = \chi' + 3BP_0^2$$

$$\text{but } \chi' = -BP_0^2$$

$$\therefore \chi'_s = 2BP_0^2 \quad \text{--- (18)}$$

2.2.5. To find a relation for the coercive field for a single domain

The relation between E and P is

$$E = \chi'P + BP^3 \quad \text{--- (14)}$$

The coercive field may be taken as the value of the field at which  $\frac{\partial E}{\partial P} = 0$

$$\frac{\partial E}{\partial P} = 0 = \chi' + 3BP^2$$

$$\text{so } BP^2 = -\chi'/3$$

$$\text{but } BP_0^2 = -\chi'$$

$$\text{so } P = P_0/\sqrt{3}$$

substituting in (14)

$$E_c = \chi'P_0/\sqrt{3} + BP_0^3/3\sqrt{3}$$

$$= -BP_0^3/\sqrt{3} + BP_0^3/3\sqrt{3}$$

$$\therefore E_c = -2BP_0^2/3\sqrt{3} \quad \text{--- (19)}$$

2.3. TO FIND A RELATION FOR THE COERCIVE FIELD FROM MASON'S THEORY.

W.P. Mason (7) developed a theory of Rochelle salt in terms of the hydrogen bonds in the crystal. By calculating the probability of a hydrogen nucleus in one potential well jumping into another he obtained a



relation between the applied field  $E$  and the dipole polarisation  $P_d$ . This theory can be applied with slight modifications to the case of KDP. The relation is then given in eqn. (11.23) ref. (19), as follows:-

$$\frac{P_d}{N\mu} = \tanh A \left( \frac{E}{\beta N\mu} + \frac{P_d}{N\mu} \right)$$

where  $P_d$  is the dipole polarisation

$N$  is the number of dipoles /cc.

$\mu$  is the dipole moment

$E$  is the applied field

$\beta$  is the Lorentz factor

and  $A = \frac{T_0}{T}$  where  $T_0$  is the Curie temperature.

Expressing the field in terms of the dipole polarisation we get:-

$$\frac{N\mu}{A} \tanh^{-1} \frac{P_d}{N\mu} - P_d = \frac{E}{\beta}$$

Taking the coercive field as the value of  $E$  for which

$\frac{\partial E}{\partial P_d} = 0$  we get:-

$$\frac{N\mu}{A} \cdot \frac{1}{1 - \left(\frac{P_d}{N\mu}\right)^2} \cdot \frac{1}{N\mu} - 1 = \frac{1}{\beta} \frac{\partial E}{\partial P_d} = 0$$

$$\therefore A \left[ 1 - \left(\frac{P_d}{N\mu}\right)^2 \right] = 1$$

$$\text{so } \frac{P_d}{N\mu} = \sqrt{\frac{A-1}{A}}$$

The coercive field  $E_c$  is then given by

$$E_c = \beta N\mu \left[ \frac{1}{A} \tanh^{-1} \sqrt{\frac{A-1}{A}} - \sqrt{\frac{A-1}{A}} \right] \quad \text{---(20)}$$

Eqn. (20) is discussed further in 4.



## 3.

METHODS OF MEASUREMENT.

Since measurements of the electromechanical constants had already been made above the Curie point, the following experiments were mainly concerned with the behaviour of the constants at, and below, the Curie point. In this region most of the constants are field dependent, so, in order to get their initial values, small fields were used throughout. For the elastic measurements, fields of less than 10 volts/cm. were used, while fields as low as 0.1 volts/cm. were used in some of the dielectric work.

3.1. MEASUREMENTS OF THE ELASTIC CONSTANTS.

The elastic constants were evaluated from the resonant frequency of longitudinal and shear modes of vibration of various crystal cuts.

In general, the vibration of a piezoelectric crystal is very complex, consisting of longitudinal, shear, torsional and flexural modes and overtones of these.

The only piezoelectric constants (on Voigt's theory) present for KDP are  $d_{14}$ ,  $d_{36}$ , which, on the application of fields  $E_x$  and  $E_z$ , produce shears according to the equations  $y_z = d_{14}E_x$ ,  $x_y = d_{36}E_z$  when external stresses are zero. Hence, only shears in the  $yz$  and  $xy$  planes are produced directly by the application of an electric field. From these the constants  $s_{44}$ ,  $s_{66}$  can be evaluated directly by the equation  $s = \frac{1}{4b^2f^2\rho}$  where  $b$  is

the breadth,  $\rho$  the density and  $f$  the resonant frequency.

This simple equation is only correct for an infinitely long and narrow crystal so a breadth correction should be applied. Atanasoff and Hart (20) have, however, shown that this can be overcome by measuring high harmonics of the resonant frequency, which has the effect of making the crystal appear very long in relation to its breadth.

Although the piezoelectric constants are such as to produce only a shear in the crystal, this can always be resolved into an extension and contraction at right angles. By cutting long bars from a plate, with their length inclined to the crystal axes, longitudinal modes are obtained. Mason (17) has shown that, by suitable dimensioning, it is possible to obtain crystals which have a negligible width correction and are free from unwanted modes. The dimensions used were of the order  $\ell = 6b = 20t$ .

Since there are six elastic constants for KDP, a minimum of six different cuts are required for their evaluation.

Equation (9b) gives for an X cut

$$S_{11}' = S_{11} \cos^4 \theta + (2S_{13} + S_{44}) \sin^2 \theta \cos^2 \theta + S_{33} \sin^4 \theta.$$

Cuts were taken at  $22\frac{1}{2}^\circ$ ,  $45^\circ$ ,  $67\frac{1}{2}^\circ$  to the  $z$  axis and their resonant frequency for lengthwise vibration was measured over a temperature range. From the formula  $s = 1/4\ell^2 f^2 \rho$ ,  $s'$  was worked out for each cut giving three

equations. On solving these simultaneously, values of  $s_{11}$ ,  $(2s_{13} + s_{44})$ , and  $s_{33}$  were found.

To find the value of  $s_{44}$ , the resonant frequency for shear vibration of a X cut crystal with its length along the z axis was measured.  $s_{44}$  was then obtained from the equation  $s = \frac{1}{4b^2f^2\rho}$  where b is the breadth of the crystal. A more accurate value was obtained by using the 3rd. harmonic.

From the value  $2s_{13} + s_{44}$  previously obtained,  $s_{13}$  was calculated.

Equation (9a) gives for a Z cut:-

$$s'_{11} = s_{11}(\sin^4 \phi + \cos^4 \phi) + (2s_{12} + s_{66})\sin^2 \phi \cos^2 \phi.$$

Cuts were taken at  $22\frac{1}{2}^\circ$  and  $45^\circ$  to the x axis and their resonant frequency for lengthwise vibration measured. The two equations obtained for  $s'$  were solved to give  $s_{11}$  and  $2s_{12} + s_{66}$ .  $s_{66}$  was obtained from the shear vibration of a crystal cut at  $0^\circ$  to the X axis and  $s_{12}$  was obtained from  $(2s_{12} + s_{66})$ . This gave all six elastic constants.

Mason (17) has shown that, when the resonant frequency of a fully plated crystal is measured, the elastic compliance at constant field  $s^E$  results. When the plating is removed and the frequency measured in an air gap holder the elastic compliance at constant displacement  $s^D$  is obtained. This is numerically equal to the value of the compliance at constant polarisation  $s^P$  within the limits of experimental error.

Instead of using an air gap holder for the measurement of the constant displacement compliances, small electrodes were placed at the centre of the crystal covering less than one tenth of the surface. The six  $s^P$  compliances were found in this way.

$s_{11}$  was found for both X and Z cuts and the values agreed within the estimated error.

Owing to the small piezoelectric constant normal to the x and y directions, the values of  $s_{44}^P$  and  $s_{44}^E$  differ by less than the experimental error.

$s_{66}^E$  might have been evaluated directly by measuring a harmonic resonant frequency of a fully plated crystal vibrating in a shear mode. It was, however, found to be difficult to make this measurement in the Curie region, so  $s_{66}^E$  was obtained as follows:-

For a Z45 bar we have:-

$$\begin{aligned} s^P &= \frac{1}{2}(s_{11} + s_{12}) + \frac{1}{4}s_{66}^P \\ \text{and } s^E &= \frac{1}{2}(s_{11} + s_{12}) + \frac{1}{4}s_{66}^E \\ \text{hence } s^E &= s^P + \frac{1}{4}(s_{66}^E - s_{66}^P) \end{aligned}$$

$s^E$  was obtained by measurements of the resonant frequency of a fully plated Z45 crystal and, from the values of  $s^P$  for the bare crystal and  $s_{66}^P$  already found,  $s_{66}^E$  was calculated. This method of measurement is liable to large errors, but the value of  $s_{66}^E$  was checked in the region above the Curie point by measuring the resonant frequency of a fully plated crystal at the 5th. harmonic and the agreement found to be within 5%.

### 3.2. MEASUREMENT OF THE DIELECTRIC CONSTANTS.

The dielectric constant of a piezoelectric crystal which is free to deform differs appreciably from that of a crystal which is rigidly clamped, on account of the piezoelectric contribution to the dielectric constant. This effect is especially marked in the case of ferroelectrics.

Measurements made at low frequencies yield the free dielectric constant. This was obtained by measuring the capacity of a crystal condenser at 2000 cycles/sec. by a bridge method described in 6.10.

Rigid clamping of a crystal to prevent any mechanical distortion is almost impossible to achieve in practice. If, however, the applied frequency is raised to a sufficiently high value, the effect of the natural frequencies and their harmonics becomes negligible. For crystals of a reasonable size, this is of the order of 10 megacycles/sec. An approximate value of the clamped dielectric constant was obtained in this way by measuring the capacity of a crystal condenser at 10 megacycles in a Q meter described in 6.11.

To obtain the dielectric measurements, crystals of dimensions 2cms. x 2cms. x 4mms. were used.

Below the Curie point the Q of the crystals was found to decrease considerably so to obtain readings on the Q meter in this region it was necessary to use smaller crystals of dimensions 4mm. x 3mm. x 1mm.



### 3.3. CALCULATION OF THE PIEZOELECTRIC CONSTANTS.

For this we use the resonant frequencies of a Z45 crystal when plated and bare.

$$\text{Since } f_P = \frac{1}{2\ell(\rho s^E)^{\frac{1}{2}}} \quad \text{and } f_B = \frac{1}{2\ell(\rho s^P)^{\frac{1}{2}}}$$

$$\text{we have } \left(\frac{f_P}{f_B}\right)^2 = \frac{s^P}{s^E} = \frac{\frac{1}{2}(s_{11} + s_{12}) + \frac{1}{4}s_{66}^P}{\frac{1}{2}(s_{11} + s_{12}) + \frac{1}{4}s_{66}^E}$$

$$\text{but equation (7d) gives } s_{66}^P = s_{66}^E - d_{36}b_{36}$$

$$\begin{aligned} \text{so } \left(\frac{f_P}{f_B}\right)^2 &= \frac{\left[\frac{1}{2}(s_{11} + s_{12}) + \frac{1}{4}s_{66}^E\right] - \frac{1}{4}d_{36}b_{36}}{\frac{1}{2}(s_{11} + s_{12}) + \frac{1}{4}s_{66}^E} \\ &= 1 - \frac{d_{36}b_{36}}{4s^E} \end{aligned}$$

$$\text{Also } d_{36} = \frac{b_{36}K_2'}{4\pi} \quad (7j)$$

$$\text{so } \left(\frac{f_P}{f_B}\right)^2 = 1 - \frac{b_{36} \cdot K_2'}{4s^E \cdot 4\pi}$$

Multiplying the values of  $b_{36}$  by  $\frac{K_2'}{4\pi}$  readily gave values for  $d_{36}$ .

From the values of  $b_{36}$  and  $c_{66}^P$ ,  $e_{36}$  was obtained by equation (6)  $a_{36} = b_{36}c_{66}^P$ .

Finally, values of  $e_{36}$  were obtained from  $a_{36}$  and  $K_2''$  by equation (7h)  $e_{36} = \frac{a_{36} \cdot K_2''}{4\pi}$

In this manner, the four piezoelectric constants were evaluated from measurements of the resonant frequency of a Z45 crystal, when plated and bare, and of the clamped and free dielectric constants.

The difference between the frequencies of the bare and plated Z45 crystals was about 0.7% of the resonant frequency at room temperature, which is not much greater than the possible estimated error of 0.6% for this

particular cut. The greater part of this error was introduced by uncertainty in the angle of cut and this was avoided by using the same crystal for the plated and bare measurements. Care had also to be taken to ensure that only a minimum of plating was used, as excess weight of plating lowered the crystal frequency.

#### 3.4. MEASUREMENT OF TEMPERATURE.

A thermocouple was used for temperature measurement and is described in 6.7.

#### 3.5. ERRORS

##### 3.5.1. Temperature.

The error in measurement of the temperature was of the order of  $1^{\circ}\text{K}$ . while changes in temperature of about  $\frac{1}{2}^{\circ}$  could be observed.

##### 3.5.2. Elastic Constants.

In calculating the elastic constants of a crystal, errors could arise in:-

- a) The measurement of the resonant frequency.
- b) The measurement of the dimensions.
- c) The angle of cut.

a) Using the General Radio Company Signal Generator Type 605B, differences of frequency could be read to 0.1%.

b) Using a micrometer screw gauge, crystals could be ground and measured to 0.01 mm. For the crystals used in lengthwise vibrations, where the resonant frequency depends

on the length of the crystal, the error was estimated at 0.1% while for shear vibrations, the error was estimated at 0.5%.

c) To estimate the percentage error caused by a  $2^\circ$  error in the orientation, the equations for rotated axes were used and the total error estimated for the frequency constant of each cut. To check the general accuracy of the work, at least three crystals were prepared for each cut and the greatest deviation from the mean was taken for the frequency constant. This is compared with the estimated error in Table 1. (page 34).

From this it would appear that the orientation error was always less than  $2^\circ$ .

Samples from crystals with tapering edges showed no measurable difference from those prepared from parallel faces, thus confirming the impression that the tapering is a purely surface effect. (see 6.2.)

The above discussion refers, of course, to the absolute accuracy of the results for the frequency constants of various crystal cuts. Since some of these are fairly sensitive to errors in orientation and since some of the constants derived from them depend on the difference between two very nearly equal quantities, the absolute errors in the magnitude of these constants may be quite large. On the other hand, the relative accuracy or scatter of points on any one graph is quite small since it depends only on frequency and temperature measurement.



Frequency, as we have seen, can be read to 0.1%, while temperature could be read to better than 1°C.

Table 1: Frequency Constant Errors.

Type of Cut.	Dimensions (mm)			Total Est. Error	Max. dev. from mean.
	l	b	t		
Z0	20.54	3.17	1.1		
	20.0	3.56	1.08	0.7%	0.33%
	12.46	3.19	1		
Z22	15.75	2.79	1.07		
	15.18	2.93	1.06	3.5%	2.6%
	13.84	3.17	1.08		
Z45	20.03	3.0	1.0		
	19.99	3.0	1.0	0.45%	0.4%
	16.78	2.5	1.03		
X0	24.35	2.97	1.07		
	23.95	2.96	1.06	0.55%	0.44%
	24.5	3.15	0.9		
X22	17.65	2.91	1.01		
	17.32	2.44	1.01	1.3%	0.2%
	21.6	2.94	0.87		
X45	12.5	2.45	1.35		
	14.55	2.4	1.01	0.5%	0.48%
	12.96	2.66	0.93		

Table II gives an estimation of the relative and absolute accuracy of the constants measured.

Table II.

Constant.	Value at Room temp.	Total Error.	Relative Error.
$s_{66}$	$15.8 \times 10^{-12}$	$\pm .15$	$\pm .05$
$s'(Z22\frac{1}{2})$	3.14	.16	.006
$s'(Z45)$	4.68	.037	.009
$s_{44}$	7.4	.037	.015
$s'(X22\frac{1}{2})$	2.225	.04	.004
$s'(X45)$	2.48	.01	.004
$s'(X67\frac{1}{2})$	2.07	.02	.003
$s_{11}$	1.6	.35	.02
$s_{12}$	- 0.14	.5	.06
$s_{13}$	- 0.55	.1	.025
$s_{33}$	1.9	.083	.01

### 3.5.3. Dielectric Constant.

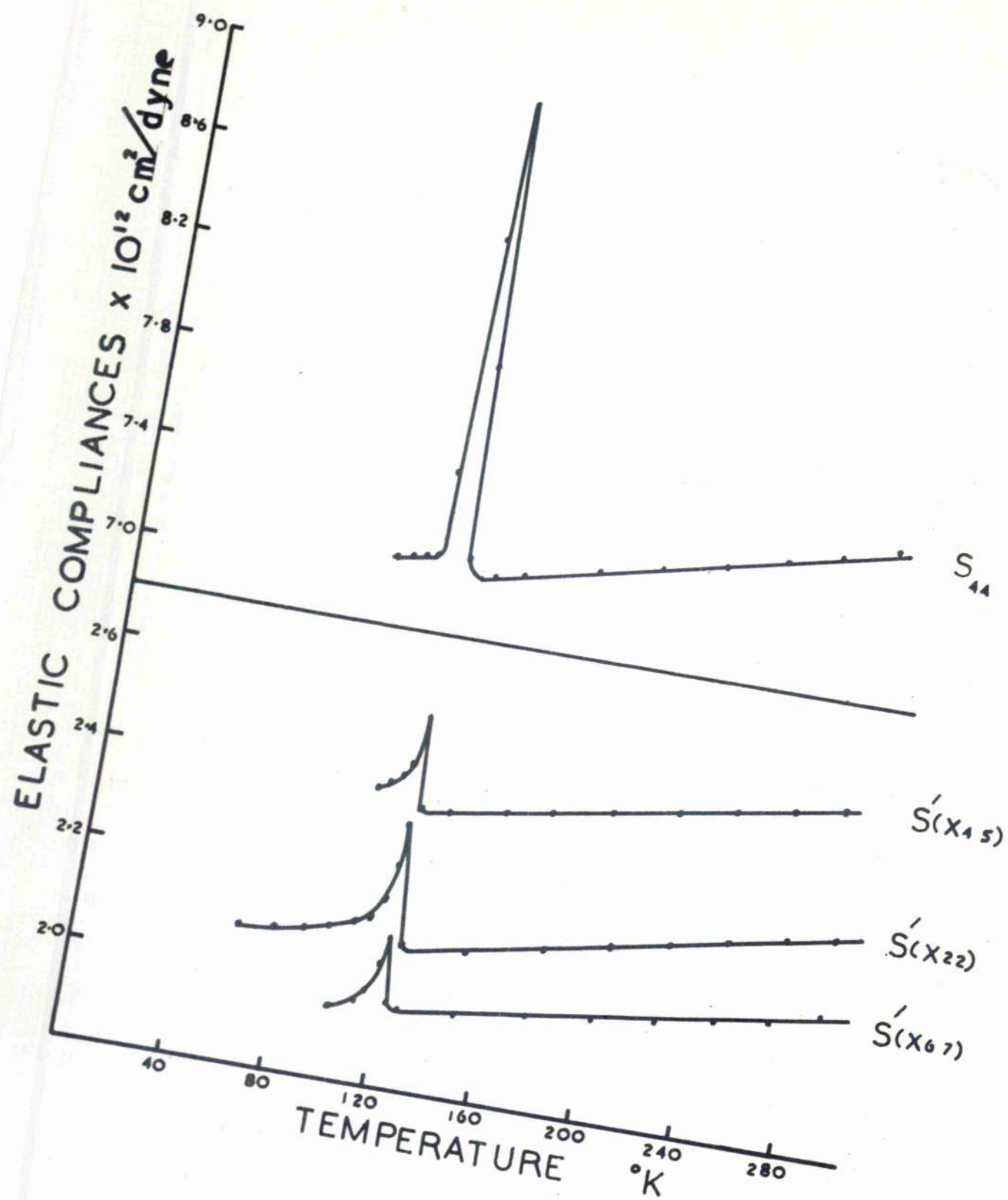
Measurement of capacity and hence of the dielectric constant could be made to an accuracy of about 2%.

However, in the region where the dielectric constant is varying very rapidly, errors in temperature measurement of 1° K might introduce an error of 20% in the dielectric constant. A number of readings taken over the steep portion of the graph showed a variation of about 10%.

The final values shown were the mean of these readings.

#### 3.5.4. Piezoelectric Constants.

The piezoelectric constants were derived from measurements of the frequency of a Z45 bar, plated and bare, and of the dielectric constants. At room temperature the difference between the frequencies of the bare and plated bars is small and the probable error consequently large. As the Curie region is approached, the frequency difference increases but the probable error in dielectric measurement also increases. At its greatest, the error in measurement of the piezoelectric constants is in the region of 10 - 15%. While this may seem to be fairly large, it compares favourably with static measurements for the piezoelectric constants of KDP where, even at room temperature, the scatter of points is about 30%. (ref. 17).

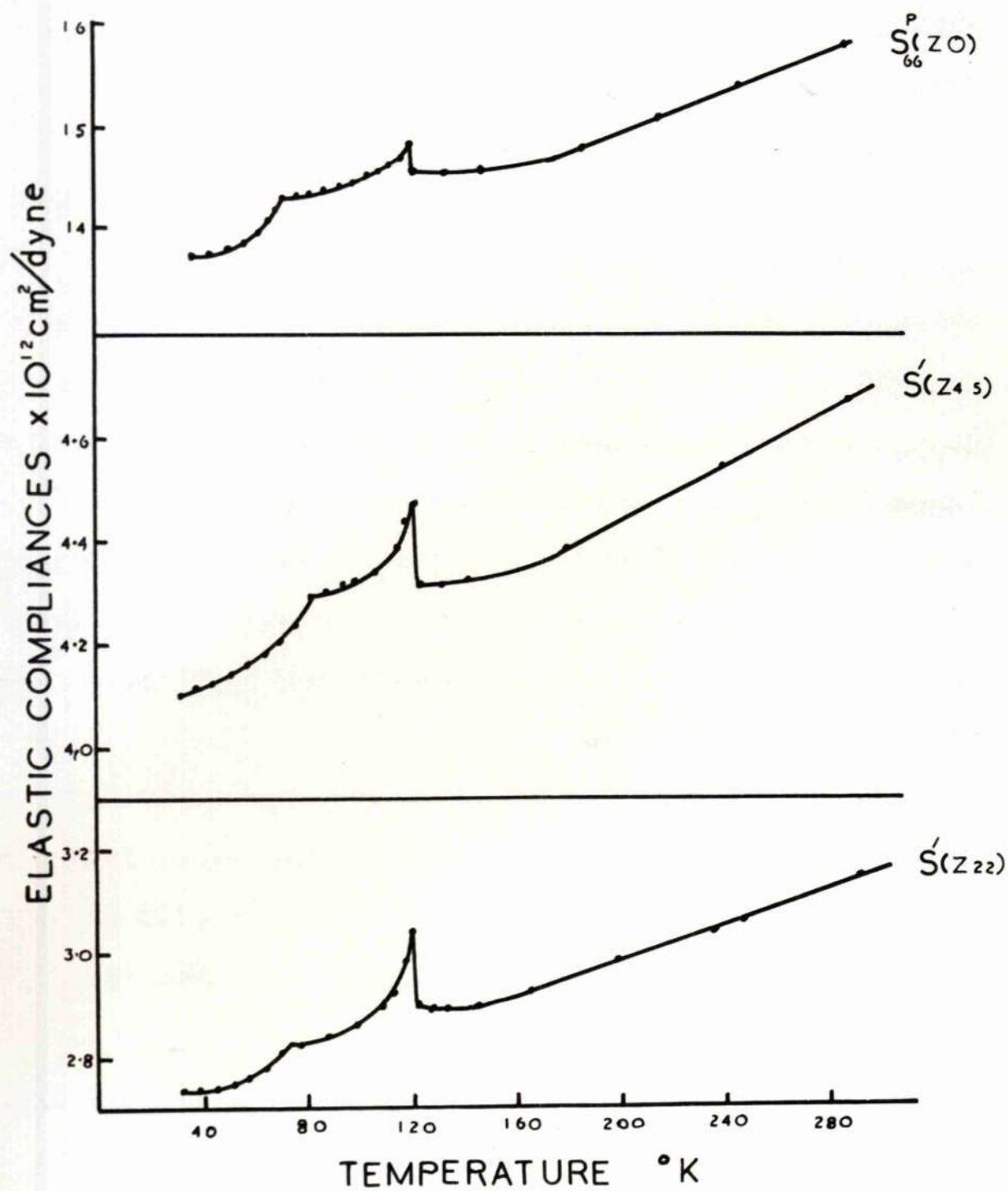


4.DISCUSSION OF THE RESULTS.4.1. ELASTIC CONSTANTS.

The values of  $s_{44}$  and  $s'$  for cuts perpendicular to the ferroelectric axis are shown on page 37. These all show anomalies at the Curie point which are greater than might be expected from comparable measurements on Rochelle salt. At a temperature of about  $121^{\circ}\text{K}$  a sharp decrease in the resonant frequency of the crystal occurs, followed by a more gradual return to a value not very different from that just above the Curie point. Thereafter, the gradient of the curve is approximately the same as that above the Curie point and shows no further anomalies down to the lowest temperature measured. The anomaly at the Curie point covers a range of about  $20^{\circ}\text{K}$ .

In measuring the constants of Rochelle salt, Mason (21) has obtained a curve giving a sharp change at the Curie point. Between the Curie points the curve follows a line parallel to the original and returns to this at the lower Curie point. The explanation given is as follows:- At the Curie point, the crystal lattice distorts and the structure, orthorhombic above the Curie point, becomes monoclinic below. This introduces new elastic constants which appear as a sharp change in the frequency of vibration of the crystal. The reverse process takes place at the lower Curie point.

This explanation does not appear satisfactory for KDP.





In the latter, after the sharp change at the Curie point, the elastic constants return slowly to approximately their original value over a temperature range in which the distortion of the crystal is known to be increasing.

(The spontaneous polarisation and shear do not reach a constant value until  $100^{\circ}\text{K.}$ )

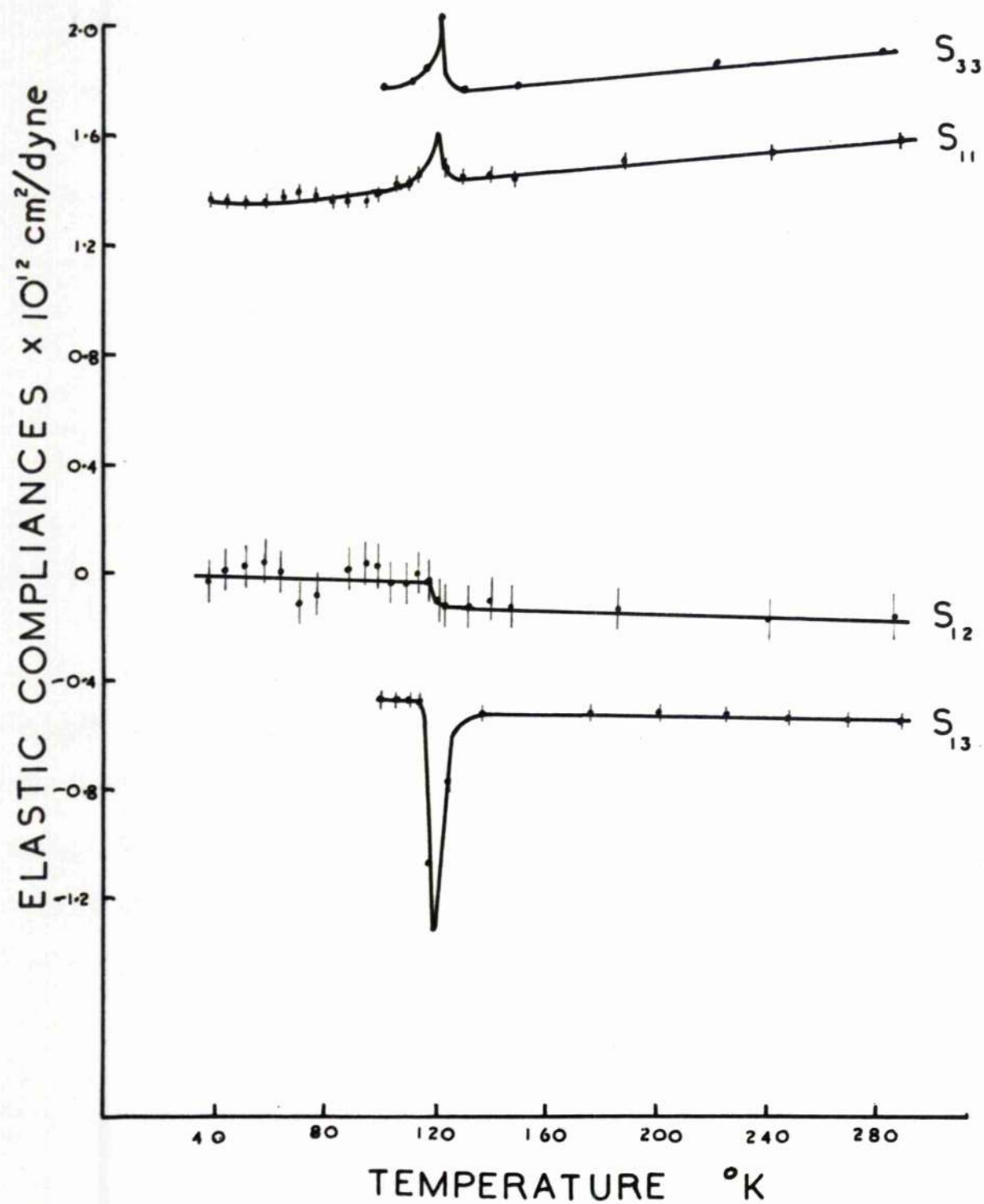
Instead, the following explanation is suggested:-

At the Curie point a spontaneous strain occurs. That is, we have a strain produced by zero stress so that the elastic compliance should become infinite. However, in the process of measurement, some stress must be applied and this prevents the compliance becoming infinite although a sharp rise in value does occur. As movement of the lattice continues to occur for about  $20^{\circ}$  below the Curie point, the compliance will only gradually return to its original value.

The curve below  $90^{\circ}\text{K.}$ , although roughly parallel to the extrapolation of the curve above the Curie point, is slightly displaced from it. This much smaller effect may very well be due to the additional elastic constants introduced by the change in structure.

It was found impossible by the method used to obtain any piezoelectric response for X cuts at temperatures below about  $60^{\circ}\text{K.}$

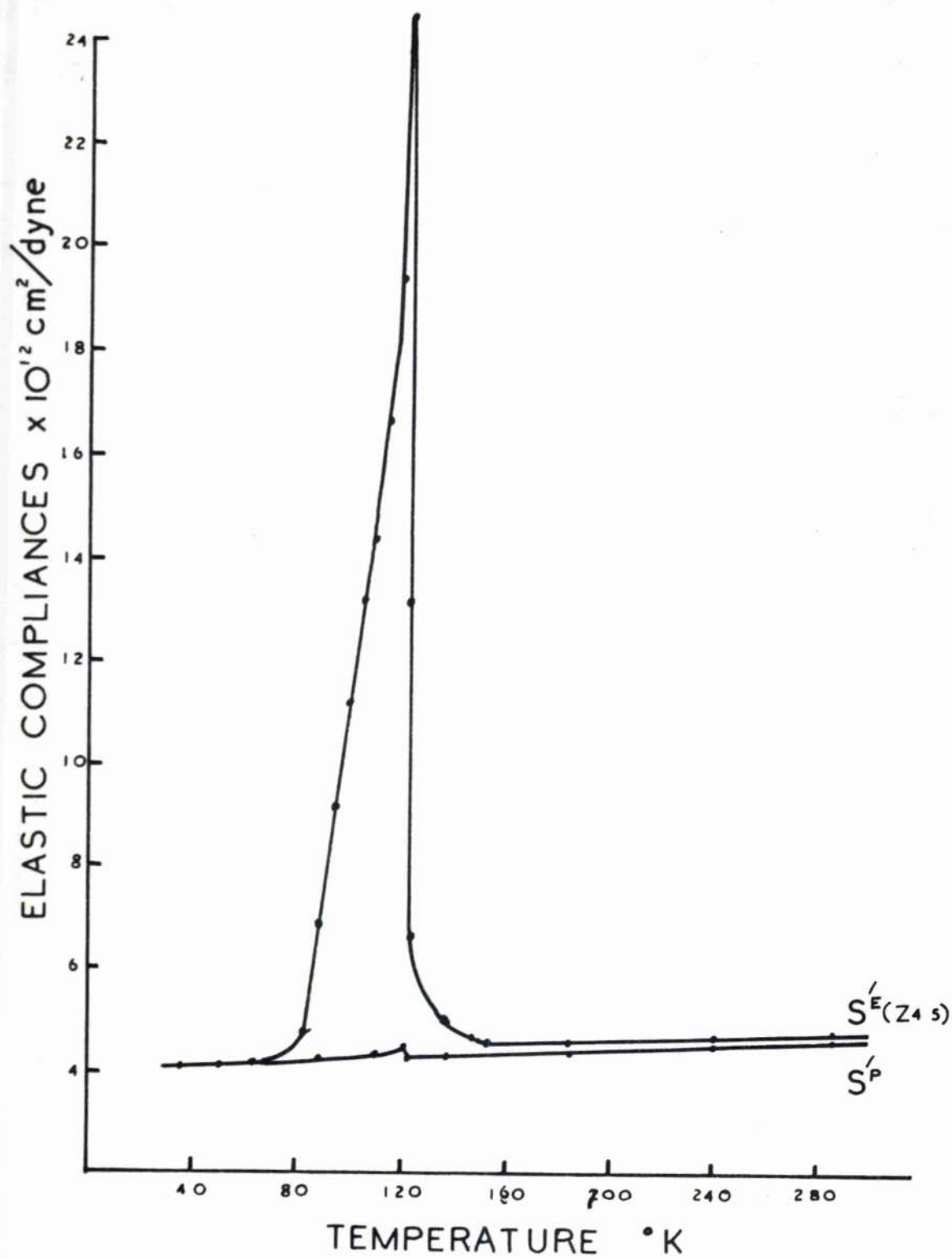
Unplated Z cut crystals showed the same sort of behaviour at the Curie point but, in addition, a change of gradient occurred between  $70^{\circ}$  and  $80^{\circ}\text{K.}$  (page 39).



Although this appeared as a small kink in the curves for  $s_{11}$  and  $s_{12}$ , (page 41) it was less than the estimated experimental error. No kink appeared in the curve for  $s'_{22}$  (page 37) which depends on  $s_{11}$ , and otherwise the values of  $s_{11}$  obtained from X and Z cuts agreed within the estimated error so it is probable that  $s_{11}$  and  $s_{12}$  have no change of gradient between  $70^\circ$  and  $80^\circ$  K. Hence the change of gradient in  $s'(Z22\frac{1}{2})$  and  $s'(Z45)$  must be due to that observed in  $s_{66}^P$ . No explanation of this effect in the curve for  $s_{66}^P$  can be given. The curves for the X cuts are shown on page 37, the Z cuts on page 39, while the calculated values of  $s_{11}$ ,  $s_{12}$ ,  $s_{13}$  and  $s_{33}$  are shown on page 41.

It will be observed that, below  $70^\circ$ , there is no trace of any further anomalies in any of the elastic constants. This, in conjunction with the evidence of De Quervain (10), who found no change of structure at a comparable temperature in  $KD_2PO_4$  by X-rays, makes it fairly certain that the sharp increase in the coercive field in the neighbourhood of  $60^\circ$  K is not due to a change of lattice or other elastic effect. It was necessary, therefore, to look for an explanation in other directions.

The measurement of the resonant frequency of a fully plated crystal, yielding the compliance at constant field, while very easy at high and low temperatures, proved to be very difficult in the region of the Curie point, both on

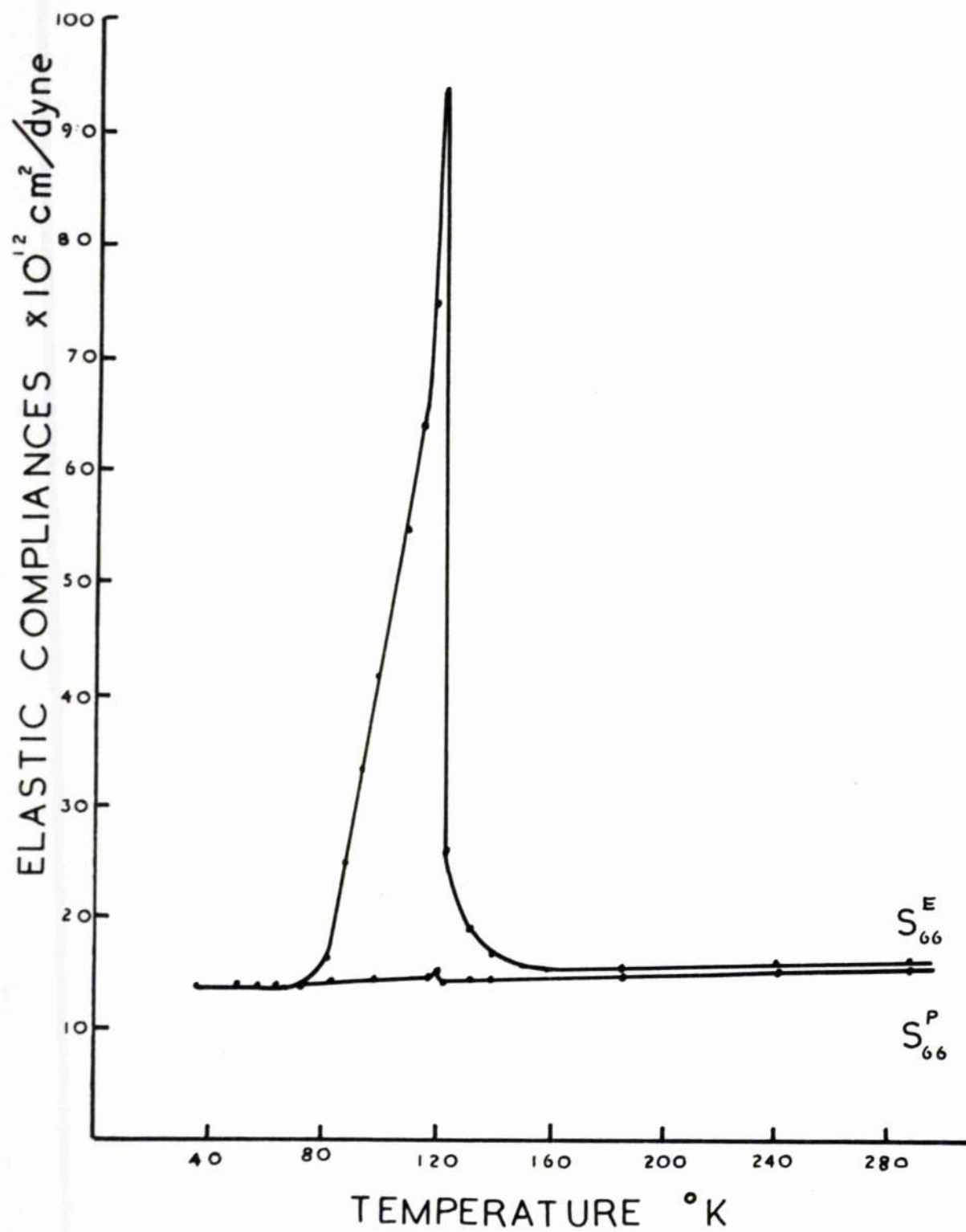


account of the large variation with temperature and the rapid increase in the dielectric constant at the Curie point. No attempt was made to evaluate completely the constant field compliances.

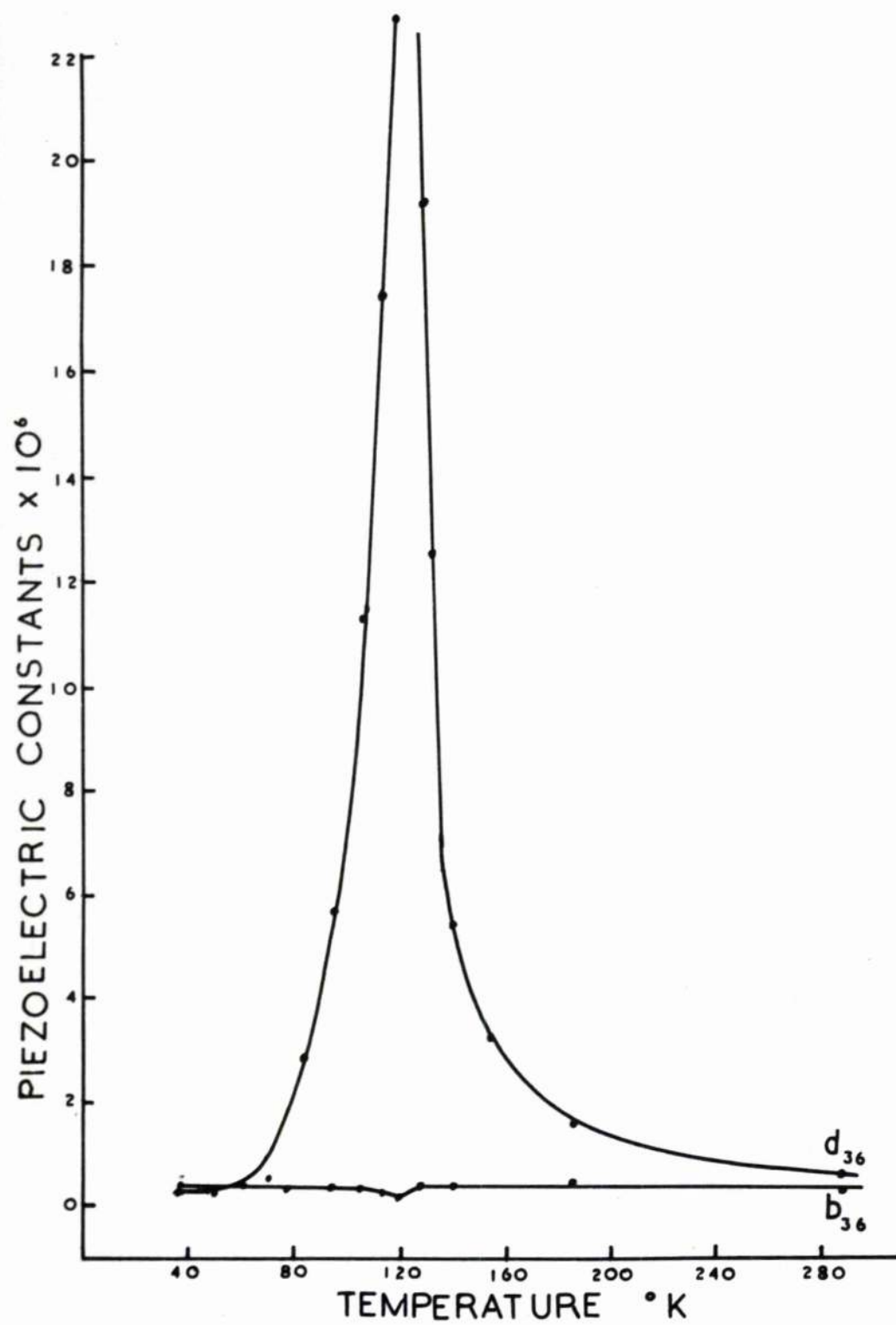
Careful measurements of the temperature dependence of  $s^E$  (Z45) were made, using the same crystal as for  $s^P$  (Z45), in order to obtain approximate values for the piezoelectric constant. These two curves are shown on page 43 drawn to the same scale, from which it will be seen that the constant polarisation compliance is practically constant with temperature compared with the constant field compliance, which varies by a factor of six on passing through the Curie point. A rough value of  $s_{66}^E$  was also obtained and plotted to the same scale as  $s_{66}^P$  on page 45. Again, the difference in the two compliances is very marked at the Curie point. These measurements indicate clearly that the compliances at constant polarisation are much more nearly true "constants" of the crystal than the compliances at constant field.

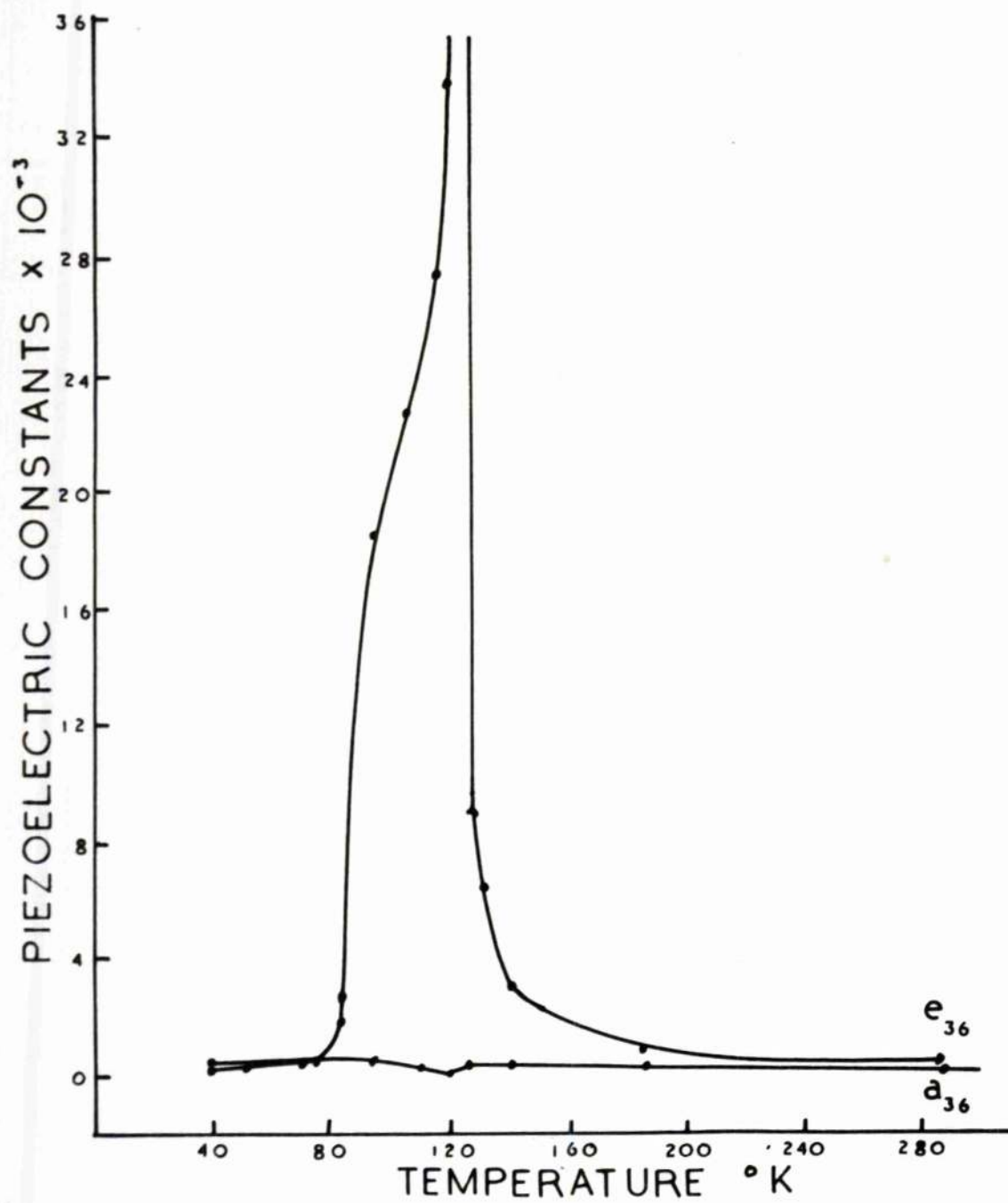
#### 4.2. PIEZOELECTRIC CONSTANTS.

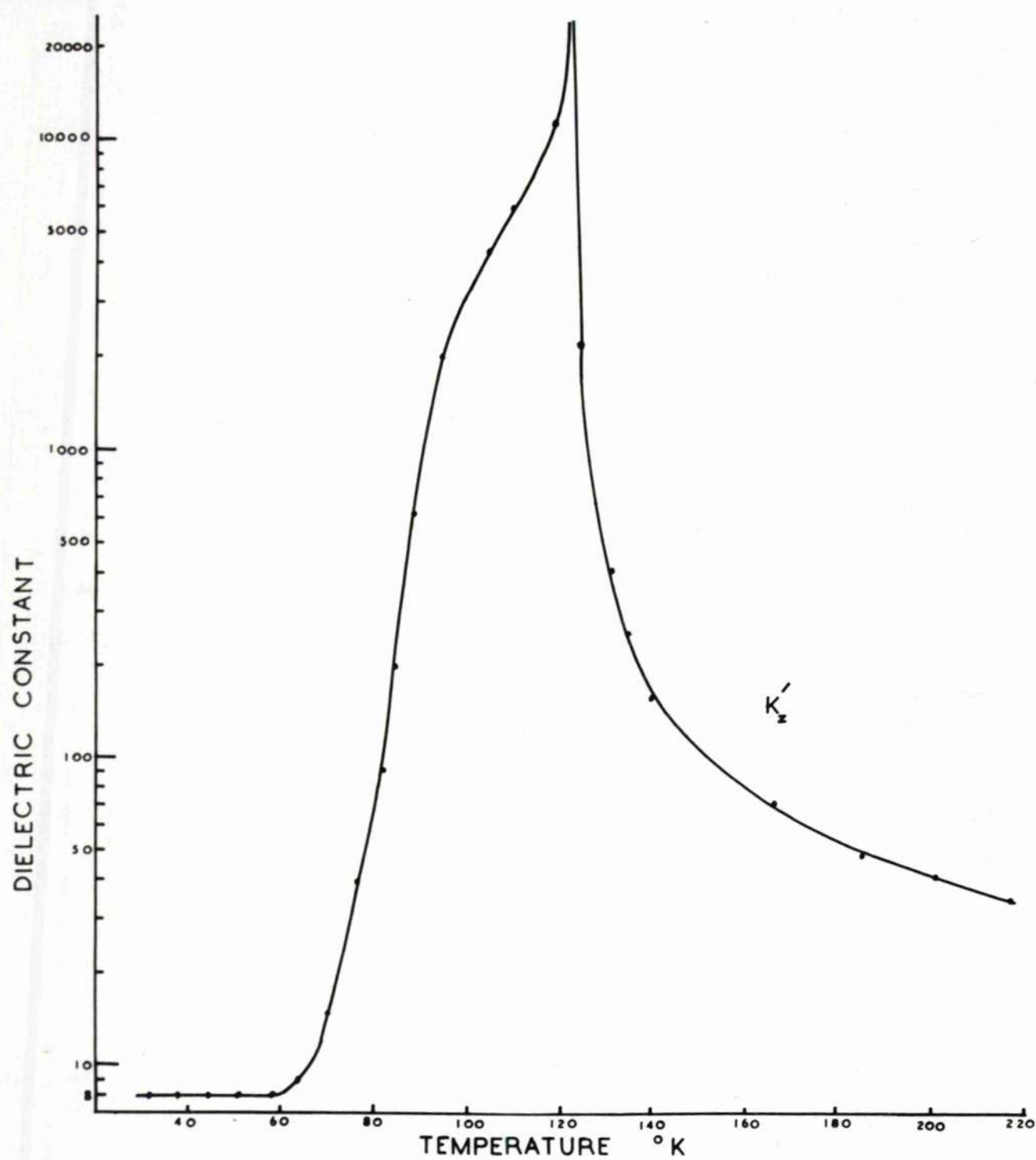
The temperature dependence of the piezoelectric constants evaluated from the compliances and dielectric constants are shown on pages 46, 47. Although, from the nature of these calculations, the accuracy is not high, the distinction between the piezoelectric constants













in terms of field strength or polarisation is at once clear. The polarisation constants show little variation in passing through the Curie point, while the field constants vary greatly.

These results, agreeing with Mueller's findings for Rochelle salt, show that, for ferroelectric crystals, the elastic and piezoelectric constants should be expressed in terms of polarisation rather than of the field used by Voigt in his original formulation.

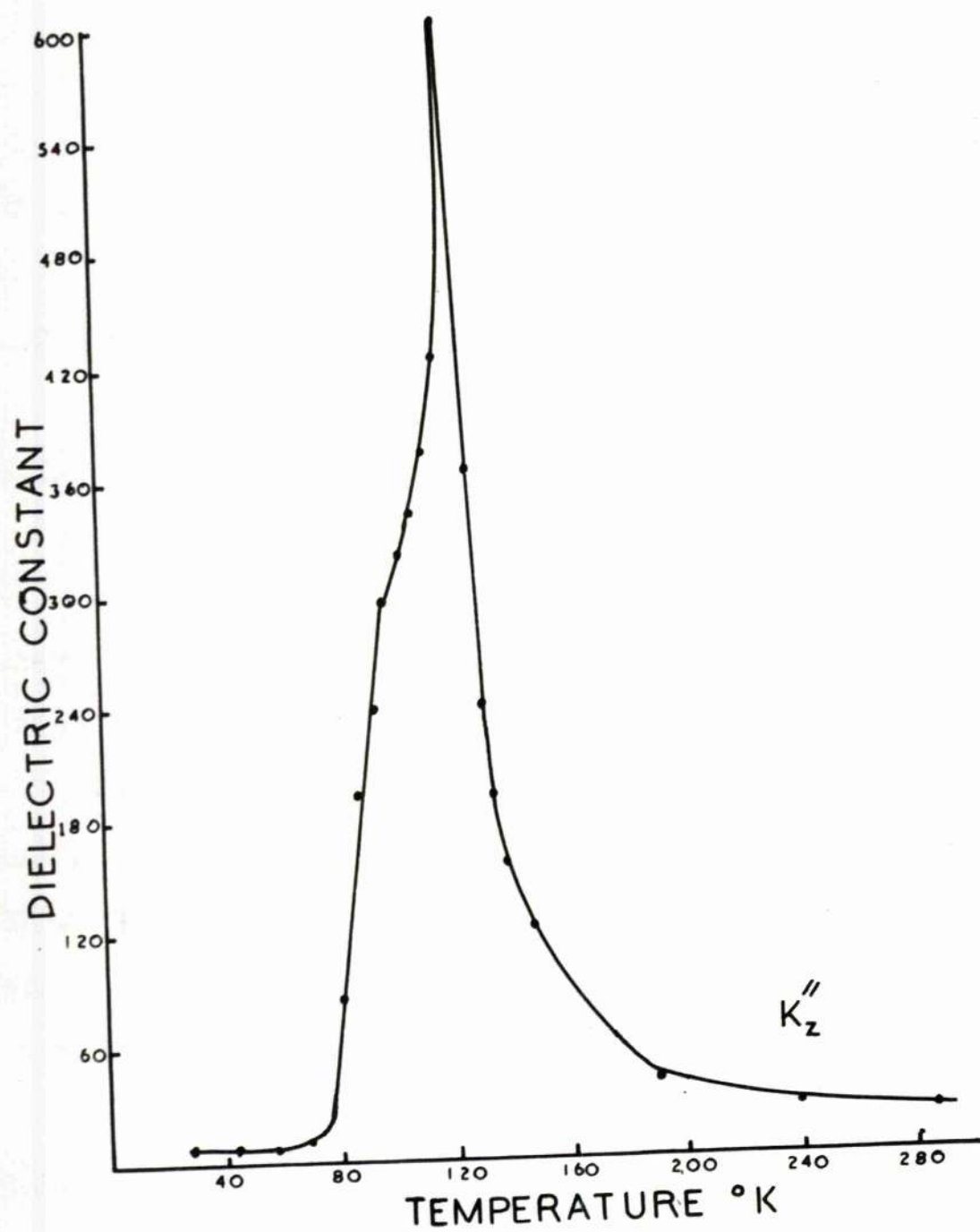
From the work on Rochelle salt, it is not clear whether the curve for  $b_{36}$  would show a decrease at the Curie point, although some effect is to be expected by analogy with the behaviour of the elastic compliances.

The present measurements show that  $b_{36}$  (and, hence, of course  $a_{36}$ ) does decrease at the Curie point, returning to approximately the same value at lower temperatures. This effect is considerably larger than the estimated experimental error.

#### 4.3. DIELECTRIC CONSTANTS.

The free dielectric constant, measured at low frequencies, is shown on page 48. At the Curie point it rises to a value greater than  $10^4$ , drops to about  $3 \cdot 10^3$  at  $100^\circ \text{K}$  and then falls more steeply to flatten out at a value of about 8 at  $60^\circ \text{K}$ .

To obtain approximate values for the clamped dielectric constant, observations were made at 10 megacycles. It had been intended to repeat these at higher





frequencies, say 20 megacycles, but unfortunately the long leads to the crystal holder, necessitated by the gas cryostat, added too much inductance to the circuit to make this possible.

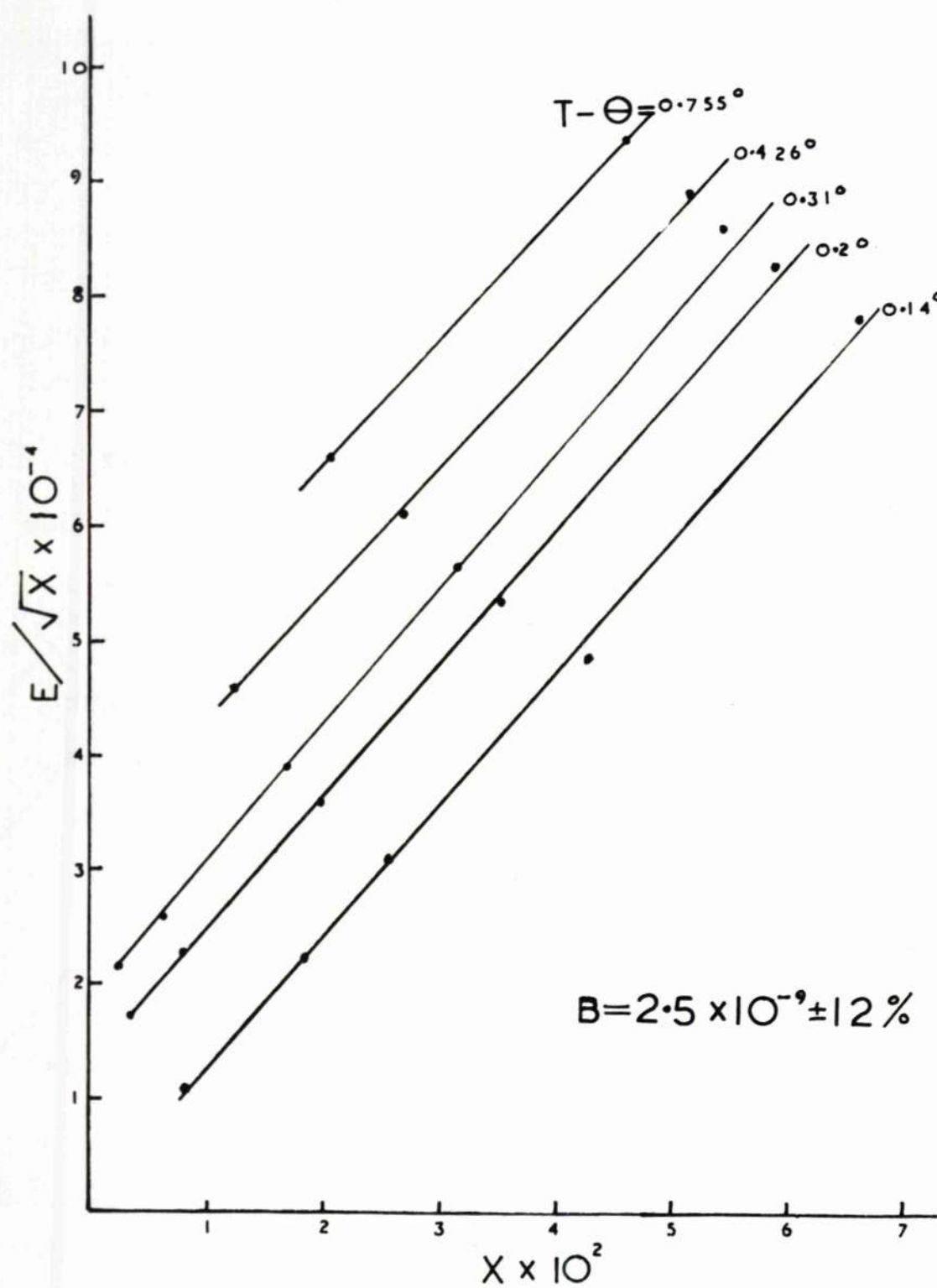
Yager (page 258, ref. 19) has found that, at room temperature, the dielectric constant measured at  $2.5 \times 10^{10}$  cycles / sec. showed no difference from the clamped value. At low temperatures the dipole relaxation frequency may be somewhat lower. Should it be as low as  $10^7$  cycles / sec., then the value obtained for the clamped dielectric constant would be less than the true value.

The curve obtained is shown on page 50. Its general behaviour is the same as that of the free constant with a pronounced change of gradient at  $100^\circ\text{K}$  and  $60^\circ\text{K}$  but with a maximum at the Curie point of only 600.

Hence, although adoption of the polarisation theory gives us elastic and piezoelectric constants which show an almost normal variation with temperature, yet the clamped dielectric constant still shows a large anomaly at the Curie point.

Two of the postulates of Mueller's theory have therefore been verified for KDP, and we shall now use his third assumption (that  $\epsilon$  requires a term in  $P^3$ ) and see whether the theory previously developed in 2.2 can be made to agree with the measurements.





#### 4.4. CALCULATIONS FROM THE PHENOMENOLOGICAL THEORY.

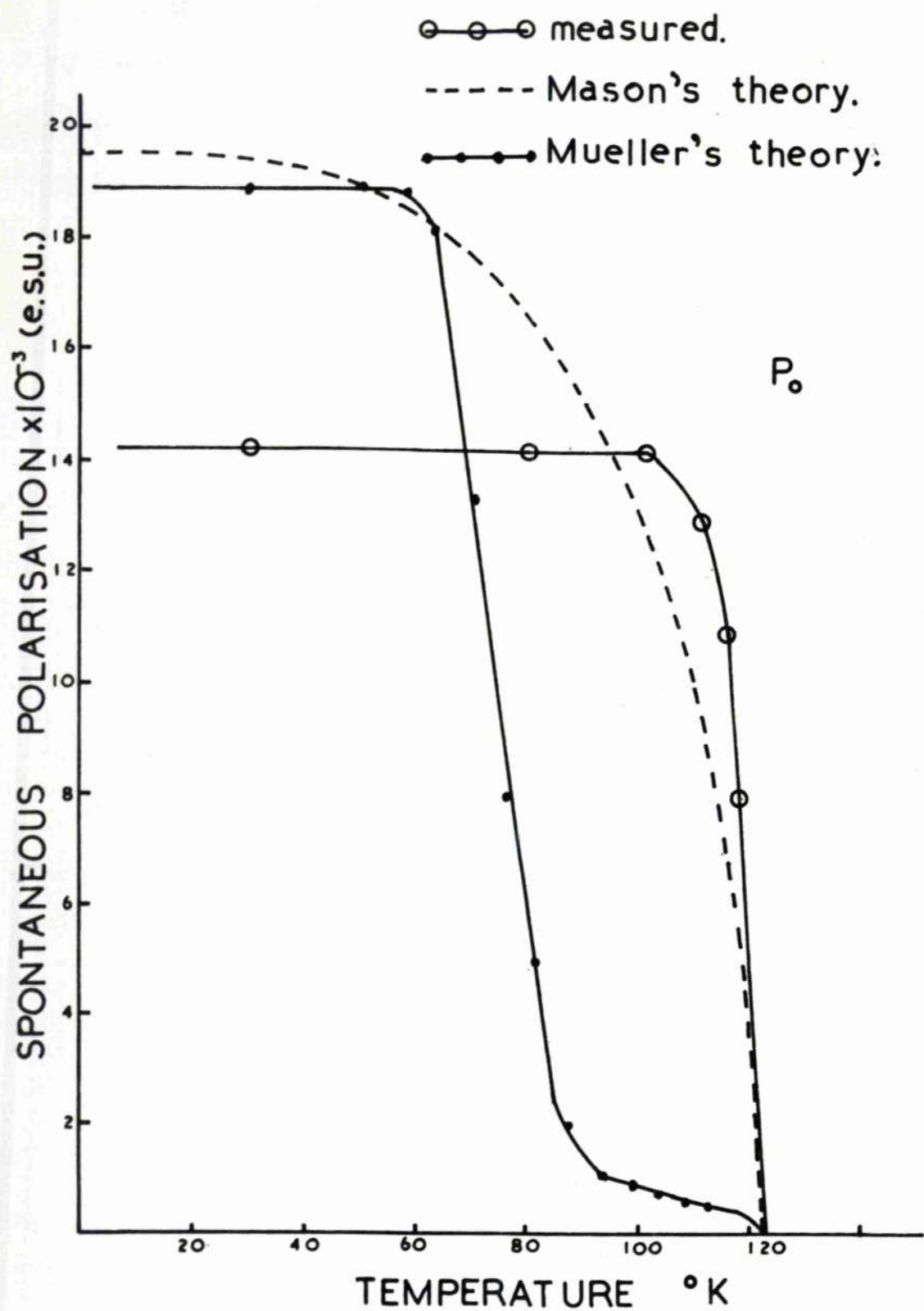
We have seen in 2.2.3. how the coefficient B may be evaluated from a knowledge of the field dependence of the dielectric constants in the region just above the Curie point. The relevant equation is  $\frac{E}{X^{1/2}} = \frac{\chi'}{(3B)^{1/2}} + \frac{X}{3(3B)^{1/2}}$  (16).

Measurements in this range have recently been made by Baumgartner (26) for different temperatures up to five degrees above the Curie point. His results are reproduced on page 63, fig.4. From these, X has been calculated and plotted against  $E/X^{1/2}$  for each temperature. The family of approximately parallel curves obtained is shown on page 52. From their gradient  $1/3(3B)^{1/2}$  the value of B was obtained and found to be  $2.5 \times 10^{-9}$ . This compares with a value of  $5.8 \times 10^{-8}$  obtained by Mueller for Rochelle salt by this method.

The spontaneous polarisation  $P_0$  may now be calculated from equation (18) which gives  $\chi'_s = 2 B P_0^2 \chi'_s$  is the reciprocal free susceptibility actually observed below the Curie point. The values of  $P_0$  obtained are compared with the measured values on page 54.

To obtain a theoretical value of the coercive field  $E_c$  we may use equation (19)  $E_c = \frac{2 B P_0^2}{3 \chi'_s}$  and the values of B and  $P_0$  obtained above. Alternatively we can use the measured value of  $P_0$ . The results are compared on page 56 with Barkla's measured values (from page 11).

The values of  $P_0$  and  $E_c$  discussed above are calculated



from the measured dielectric constant. We can, however, reverse this process and, using the measured value of the spontaneous polarisation, calculate a value of the clamped dielectric constant below the Curie point.

From eqns. (7f)  $\chi_z'' = \chi_z' + a_{36} b_{36}$

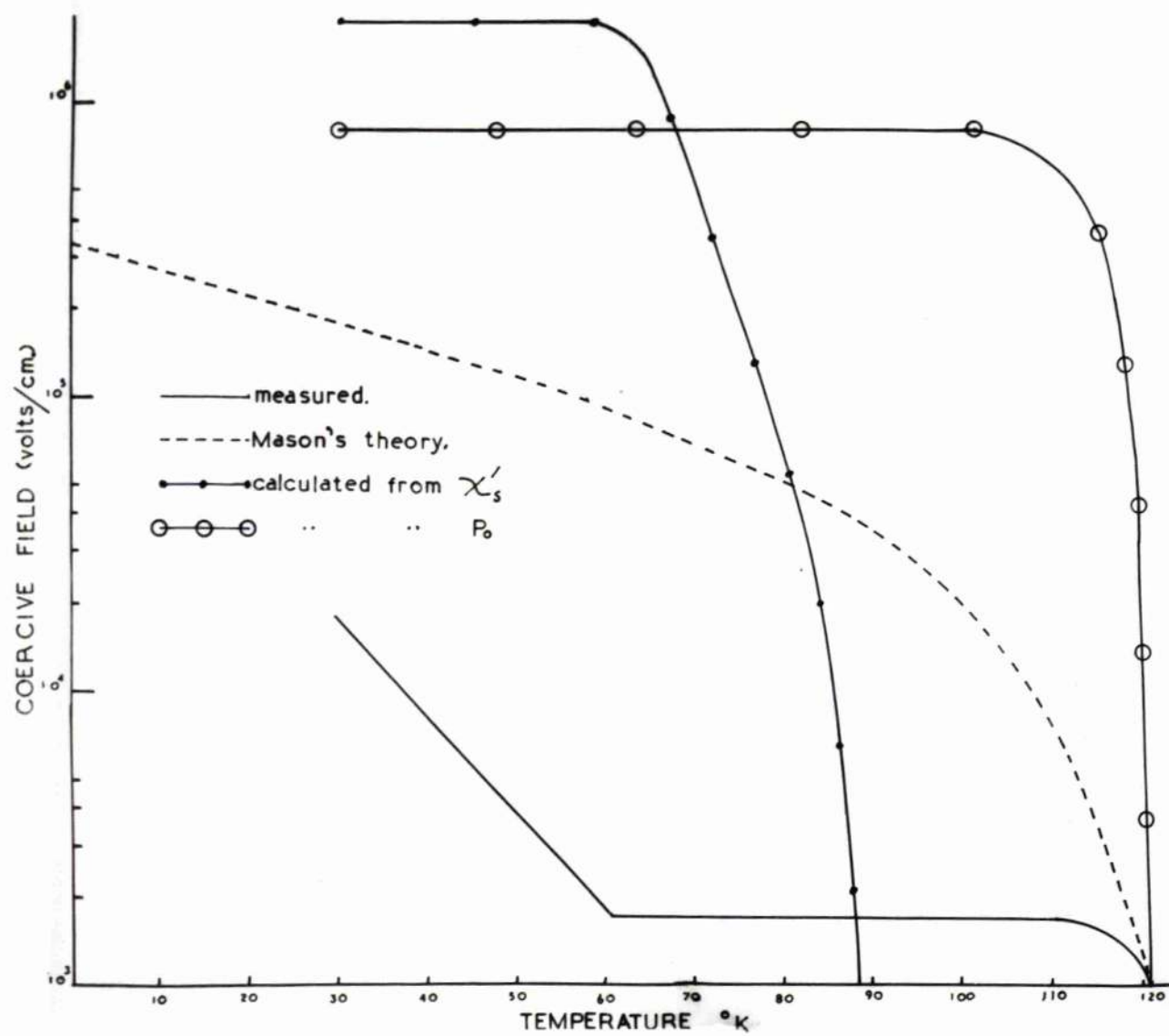
and (18)  $\chi_s' = 2BP_0^2$

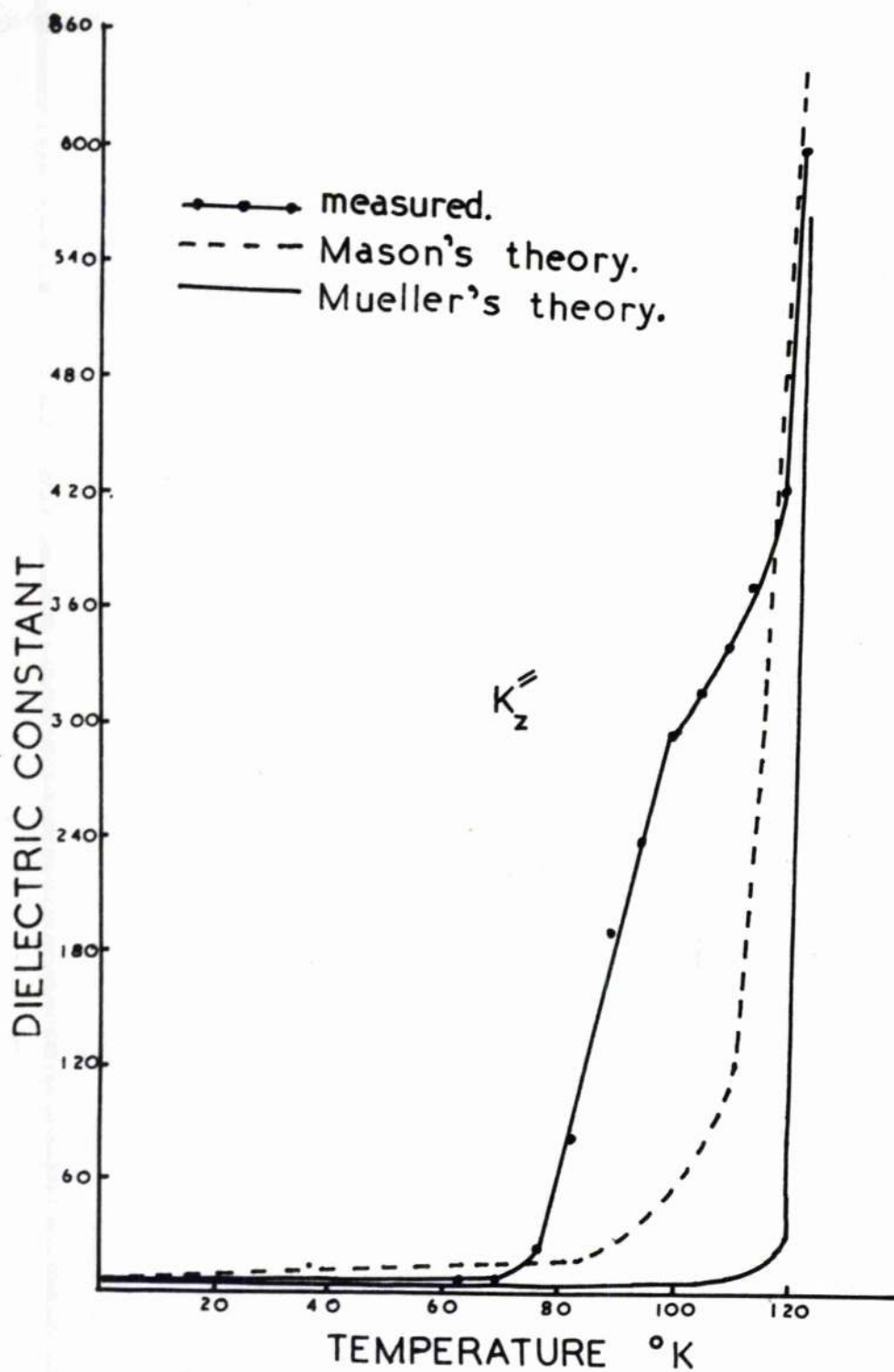
we get  $\chi_z'' = \frac{4\pi}{K_z'' - 1} = 2BP_0^2 + a_{36} b_{36}$

and from this  $K_z''$  can be obtained. The results are compared with the measured values on page 57.

#### 4.5. CALCULATIONS FROM MASON'S THEORY.

Mason (19) has developed a theory for Rochelle salt and KDP in terms of the motion of the hydrogen atoms between potential wells along the hydrogen bonds, thus obtaining expressions for the dielectric constant and spontaneous polarisation. Using data obtained from the temperature dependence of the dielectric constant above the Curie point, he calculates values for the spontaneous polarisation. This is compared with the measured values on page 54. It will be observed that the measured curve flattens off at about 100°K. Mason suggests that this is due to the failure of the applied field to line up all the domains. His value of the saturation polarisation of  $19.5 \times 10^3$  e.s.u. agrees remarkably well with the present value of about  $19 \times 10^3$  e.s.u., obtained from the phenomenological theory using the field dependence of the dielectric constant above the Curie point.







The clamped dielectric constant was calculated from Mason's formula and is shown plotted on page 57.

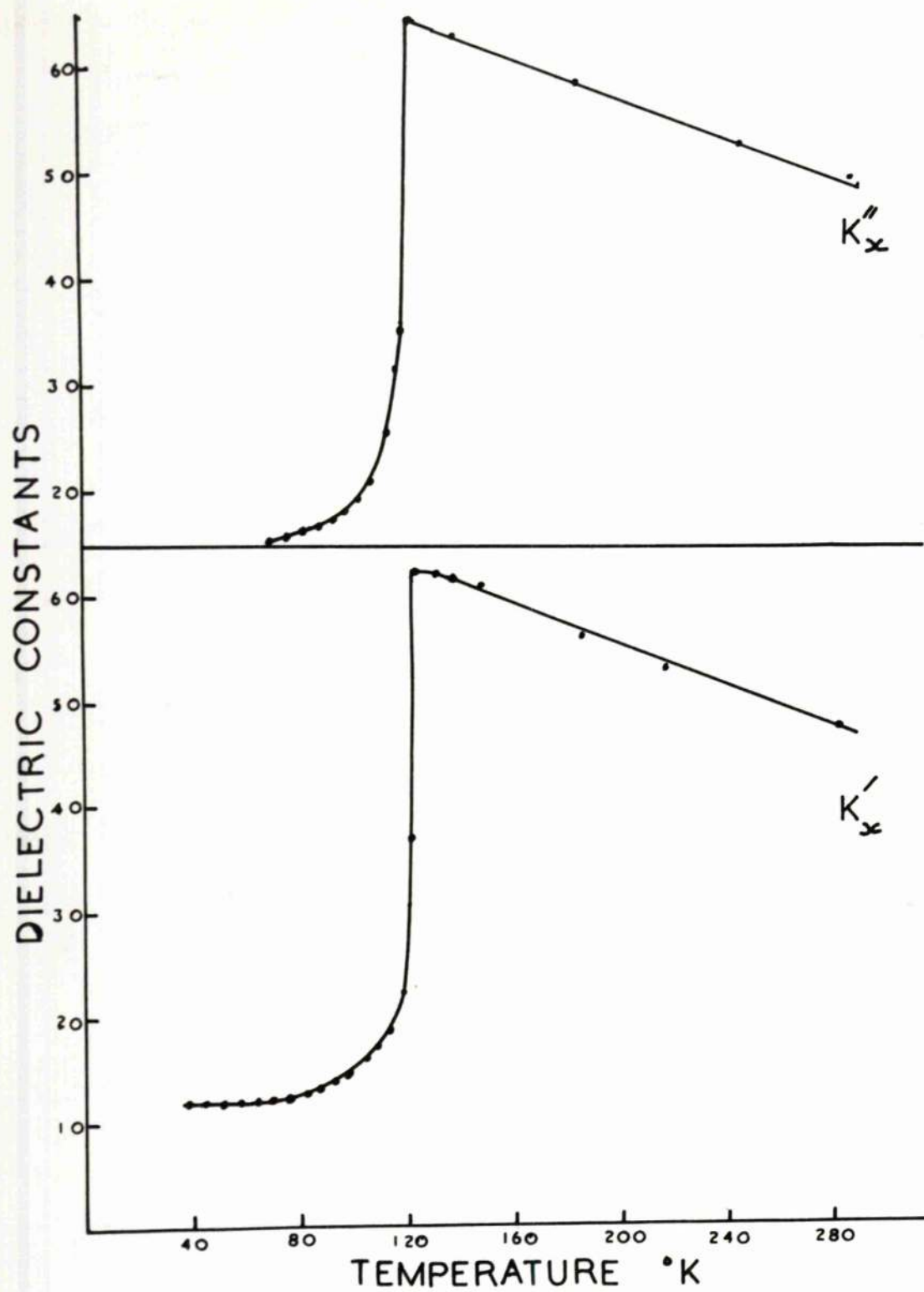
In his book (19) Mason does not work out in detail the coercive field for KDP but, using an approximation which is valid for Rochelle salt, he concludes that as the temperature tends to zero the coercive field should tend to infinity, thus explaining the high coercive field at low temperature.

From his equation relating polarisation and field, an expression for the coercive field is derived in 2.3. From this and his curve for the spontaneous polarisation, values for the coercive field were calculated and are shown plotted on page 56. It will be observed that the curve reaches a definite limit at the absolute zero; consequently, it would appear that Mason's conclusions on this point are incorrect.

#### 4.6. THE FREE AND CLAMPED DIELECTRIC CONSTANTS $k_x$ .

The dielectric constant measured at right angles to the ferroelectric axis at high and low frequencies is shown on page 59. Little difference in behaviour is observed between the clamped and free values, as might be expected from the small piezoelectric coupling in this direction. The fact that there is a maximum at the Curie point contrasts with the behaviour of Rochelle salt, where the equivalent constants remain at a steady, low value of about 9 and 11 respectively.

The sharp drop in the value of  $k_x$  at the Curie



point can be explained as being due to the fact that, at this temperature, most of the dipoles are lined up along the c axis and so a field along a direction at right angles will have very little effect. In fact however, the curve does not finally flatten out until about  $60 - 70^{\circ}\text{K}$ .

#### 4.7. GENERAL DISCUSSION.

Considering first the curves for the spontaneous polarisation shown on page 54, it will be seen that both theories indicate a much higher saturation polarisation than that actually observed. Mason's suggestion that some of the domains may be very difficult to reverse might account for this difference.

Much more serious is the divergence between the general shape of the observed polarisation curve and that calculated from dielectric constant measurements. The latter remains at a very low value until about  $90^{\circ}\text{K}$  and then rises steeply to flatten off at about  $60^{\circ}\text{K}$ .

Now, the spontaneous polarisation has been obtained from saturated hysteresis loops by a number of observers, and their results, though differing in detail, do in general conform to the curve shown. Also, the angle of distortion has been measured down to  $77^{\circ}\text{K}$  (28) and again the results confirm the behaviour of the spontaneous polarisation. It seems, therefore, very unlikely that the values of spontaneous polarisation can be far wrong.

The calculated coercive field shown on page 56 is, of course, for a single domain, and we should expect it to be higher than that actually occurring in a multi-domain crystal. Its behaviour, however, is in direct contrast to that of the observed field, rising steeply where the latter is steady and flattening out where the latter begins to rise steeply. The agreement with the Mason theory curve is likewise poor.

It can, of course, be argued that Mueller's introduction of a term in  $P^4$  to the energy equation has no great theoretical justification and that, although it rendered reasonable agreement with experiment for Rochelle salt, a more complex function might be necessary for KDP.

It could also be said that the value obtained for B might be wrong by a considerable factor and that, even if correct above the Curie point, it might vary considerably on passing through the Curie point.

Granted all this, it is difficult to see how any function, however complex, could bring the calculated and observed values of  $P_0$  to agreement, since below  $100^\circ\text{K}$  the polarisation remains practically constant, while the dielectric constant drops from the region of 4000 to about 8 at  $60^\circ\text{K}$ . We are, therefore, forced to the conclusion that the dielectric constant, measured below the Curie point, bears no relation to the spontaneous polarisation.

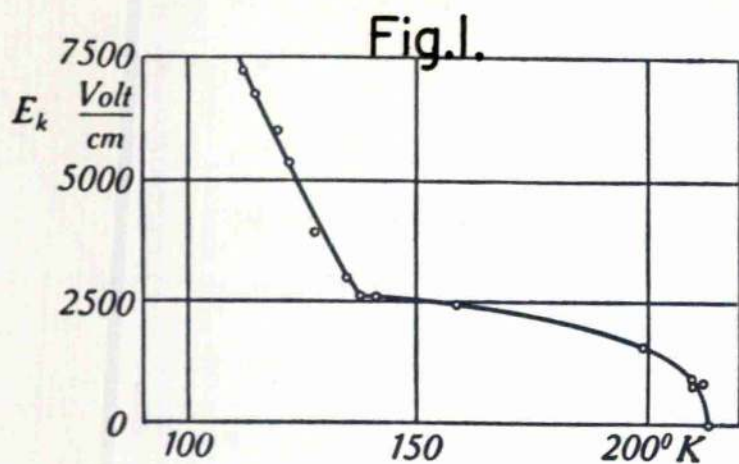
That the high dielectric constant at, say,  $100^\circ\text{K}$  could be due to the reversal of domains is scarcely possible,

for field strengths were used down to 0.1 volts/cm., while at this temperature the coercive field is in the neighbourhood of 2000 volts/cm.

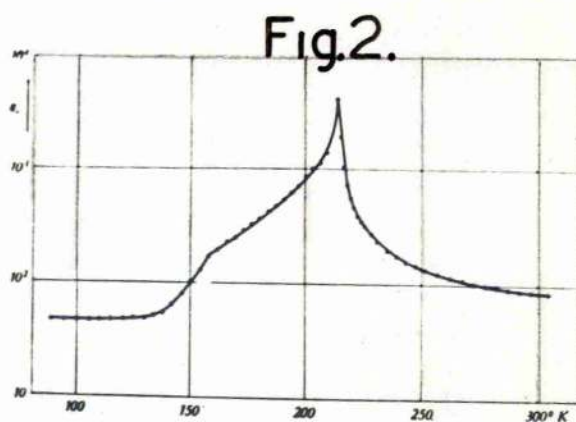
The dielectric constant is, however, slightly field dependent even at very low field strengths. For example, a change in field strength from 1 volt/cm. to 0.1 volt/cm. produced a decrease in dielectric constant of about 6%.

It will be recalled that, in the case of ferro-magnetics, it is possible, in suitable samples, to obtain a large magnetisation by the application of very small fields. At the boundary between two domains, instead of having two adjacent dipoles pointing in opposite directions, there is a gradual change in the direction of the dipoles occurring over many atomic planes. In certain specimens a small field may then be able to move these "Bloch walls" in a direction transverse to itself for considerable distances. Presumably, in a perfect crystal this would mean that a very small field could magnetise the specimen to saturation. Impurities and other imperfections in the lattice will prevent this occurring and fields large enough to reverse complete domains without wall movement may be required. The initial permeability is, therefore, intimately connected with the coercive field in the magnetic case. Their relation is shown on page 63, fig.3, from which it will be observed that, in a large variety of substances, high initial permeability is associated with low coercive field and vice versa.

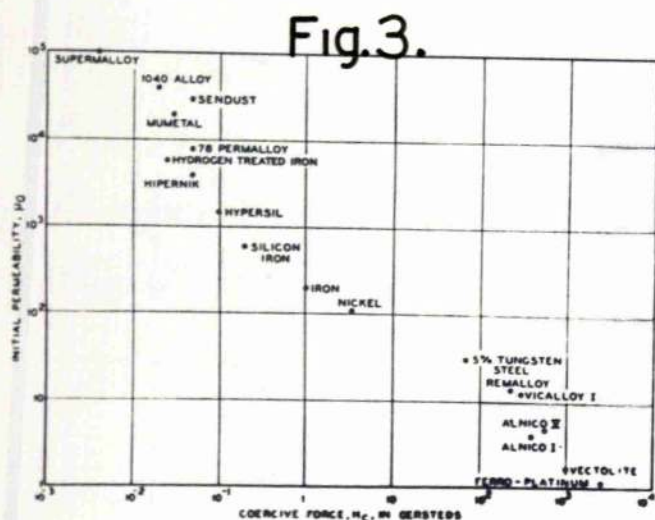




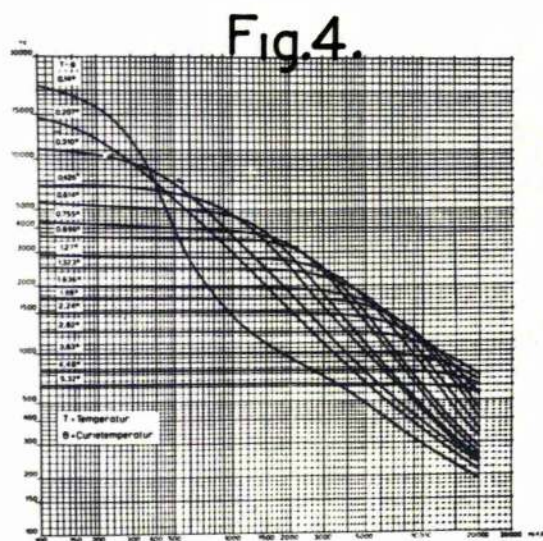
Coercive field—Temp.  
in  $\text{KD}_2\text{PO}_4$  (ref.15).



Diel.const.—Temp.  
in  $\text{KD}_2\text{PO}_4$  (ref.22).



Init.perm.—Coercive field.  
in Ferromagnetics (ref.25)



Diel.const.—Field.  
in  $\text{KH}_2\text{PO}_4$  (ref.26)



With this picture in mind, the behaviour of KDP becomes more clear if we assume that, as well as the complete reversal of domains by large fields, we can have movement of the domain wall. Somewhere in the region of  $100^{\circ}\text{K}$  the spontaneous polarisation has reached the maximum and, hence, the high dielectric constant below this point must be due to small movements of the domain walls. As the temperature falls, this wall movement becomes more difficult until at about  $60^{\circ}\text{K}$  it has almost ceased, since below this temperature the dielectric constant changes very little. To polarise the substance in a given direction, then, requires reversal of complete domains, so we have a sharp increase in the value of the coercive field.

The intimate relation between the dielectric constant and coercive field can also be seen in the behaviour of  $\text{KD}_2\text{PO}_4$ . Bantle (22) measured the dielectric constant at a field strength of 40 volts/cm. His graph is reproduced in fig. 2, page 63, and shows the dielectric constant becoming independent of temperature at about  $140^{\circ}\text{K}$ . Zwicker and Scherrer (15) obtained a plot of the coercive field with temperature, reproduced in fig. 1, page 63. A sharp increase in the coercive field occurs at about  $140^{\circ}\text{K}$ , which corresponds very closely to the temperature at which the dielectric constant becomes independent of temperature.

A further point of interest in Bantle's curve is the

kink which occurs at about  $160^{\circ}\text{K}$ , corresponding to the kinks in the KDP curves at about  $100^{\circ}\text{K}$ . Thus, for both KDP and  $\text{KD}_2\text{PO}_4$  the kink in the dielectric constant curve appears to occur in the neighbourhood of the temperature at which maximum polarisation is reached.

No direct observations of the domain structure of KDP have yet been made but recent work on barium titanate has dealt with this subject. Forsbergh (27) claims that movement of domain walls can be seen by use of a polarising microscope. The wall movement is said to respond smoothly to field until the field is of sufficient magnitude to reverse complete domains. Unfortunately, no information is given as to the magnitude of the fields required to obtain movement of the domain wall.

It may be noted in passing that the phenomenological theory developed by Devonshire (11) for barium titanate yields dielectric constants considerably less than those actually observed. The evidence from barium titanate lends weight to the supposition that the behaviour of the dielectric constant and coercive field in KDP can be accounted for by movement of the domain wall.

Difficulties arise when we try to visualise something similar to a Bloch wall. In ferromagnetism a magnetic dipole can assume any direction in space, so the gradual turning round of the dipole direction required for the Bloch wall can be achieved. In KDP no such effect seems to be possible since the dipole can only orientate itself

along six directions (assuming the basis of Slater's theory to be correct).

Suppose, first of all, that the adjacent molecules forming the boundary of two domains have dipoles pointing in opposite directions. Then on the bond between them there must either be two hydrogens or none at all. This is scarcely possible as it would require movement of hydrogen atoms from one bond to the next at the Curie point, unless bonds with two or no hydrogens exist in appreciable numbers at all temperatures.

Next, suppose we have a buffer layer of molecules with the dipoles on one side pointing up and on the other pointing down. Then the buffer dipole will have one hydrogen up and one down so its dipole will point at right angles to  $c$ . Below the Curie point all dipoles prefer to lie along the  $c$  axis so the boundary dipole will be in an unstable position and can readily be turned into either the  $+$  or  $-c$  direction by a small field, thus providing a mechanism for the movement of the boundary walls.

If this were the whole story, of course, complete polarisation of the crystal could be accomplished by very small fields, but as we have seen, the field required at  $100^{\circ}\text{K}$  is of the order of 2000 volts/cm. This can be accounted for, if we consider that the domain walls can be moved transversely by a small field, only until an obstacle is reached in the form of an impurity or dislocation in the crystal. The coercive field is a

measure of the force required to overcome this obstacle.

Dipoles at right angles to the c axis will not be able to persist to absolute zero, so a temperature will be reached at which the easy method of polarisation by domain wall movement is no longer possible. This temperature will appear macroscopically as the point at which the dielectric constant becomes independent of temperature and the coercive field increases towards the theoretical value for a single domain.

The behaviour of the KDP dielectric constants at right angles to the ferroelectric axes fits in with this general picture.  $K_{\perp}$  (page 59) does not reach a constant value until 60 or 70° K suggesting that, down to this temperature, dipoles can still be orientated along the a or b axis. Unfortunately, the accuracy of measurement is not sufficient to determine whether the gradient of the  $K_{\perp}$  curve vanishes completely below 60° K.

To summarise the above suggestions to account for the variation of the dielectric constant with temperature, we may say that, had the transition been one of the first order, as predicted by Slater's theory, all domains would be completely polarised at the Curie point. No further movement of dipoles would then be possible without the application of very large fields and, consequently, the initial value of the dielectric constant would fall rapidly from the high value at the Curie point to a constant low value due to atomic and electronic

polarisation only. Two effects completely mask this behaviour. In the first place, the transition is not sharp and the spontaneous polarisation does not reach a constant value until  $20-30^{\circ}$  below the Curie point. When this temperature has been reached and the lining up of dipoles in the domain has been completed, the dielectric constant drops more rapidly but, because of the dipole movement due to motion of the domain wall, it does not reach its final small value until  $60^{\circ}$  K.

With this in mind the poor agreement of the Mason and Mueller theories with experiment cannot be taken as a condemnation of the theories, for they apply only to a single domain. Likewise, no valid objection to the Slater theory has been presented, although the broadening of the transition has not yet been satisfactorily explained.

#### 4.8. POSSIBLE FUTURE RESEARCH.

It is thought that further progress in the understanding of ferroelectrics will best be achieved by a development of domain theory and experiment to a level comparable with that obtaining in ferromagnetism. Attempts might be made to study the domain structure of KDP directly by the polarising microscope although this approach is likely to be much more difficult than in the titanate case. Electro-optical studies might also prove worthwhile. Comparison of the low temperature behaviour



of other ferroelectrics of this group (e.g.  $\text{KH}_2\text{AsO}_4$ ) would be interesting. No systematic high frequency dielectric studies have yet been attempted. The relaxation time of the KDP dipole and its relation to temperature might help to throw light on the mechanism of polarisation. If necessary this study could be extended into the infra-red.



5.CRYSTAL GROWTH.5.1. THE SEARCH FOR A SUITABLE TECHNIQUE.

It was known that crystals of potassium dihydrogen phosphate (KDP) could be grown from small seeds set in a saturated solution which was then slowly cooled; it was also known that seeds could be produced by allowing a saturated solution to cool down rapidly.

First attempts to obtain small seeds produced a mass of small needle-shaped crystals but the addition of a small amount of KOH gave small, short prisms, Ludy (23). The majority of these were misshapen or cracked, but out of a fairly large number a few which were well-shaped and free from flaws could be obtained. These were used as seeds.

The seed was drilled and mounted on a small pin fixed vertically near the perimeter of a 2" diameter horizontal perspex disc driven at about 10 revs/minute from a small clock motor. The disc and seed were immersed in a saturated solution of KDP contained in a glass dish holding less than a litre of solution. This in turn was immersed in a water bath.

The temperature was controlled as follows. A small bobbin of platinum wire was immersed in the bath, forming one of the arms of a Wheatstone bridge with a wall galvanometer as its detector. When the bridge was balanced the light reflected from the galvanometer mirror

fell on a photoelectric cell. The output of the cell, after amplification, controlled a thyatron with the bath heater in its anode circuit. The circuit was arranged in such a way that, when the temperature fell the spot of light moved onto the photocell and thus started off the heater. By this means, a temperature regulation of rather better than  $0.1^{\circ}\text{C}$  could be maintained. By altering the balance of the bridge, the bath temperature could be decreased slowly.

With this arrangement, a crystal about 3 cms x 1 cm. x 1 cm. was ultimately grown but, although its external shape was good, it was internally cracked and completely unsuitable for elastic measurements.

Up to this point, the amount of solution used had been too small to produce large crystals by cooling over, say, a  $20^{\circ}\text{C}$  range. In addition, the poor quality was attributed to temperature gradients in the solution.

Next, attempts were made with quantities up to three litres. The heating was now done from the mains and controlled through a relay by the thyatron current.

Trouble was now experienced from a large quantity of nuclei forming near the surface of the solution and falling towards the bottom; many of them, landing on the growing crystal, spoiled its quality. To counteract this, crystal seeds were drilled and suspended by hairs from a paxolin disc 4" in diameter, in the hope that the disc would collect most of the falling nuclei. The

crystals produced, while improved in quality, were by no means good.

The resistance thermometer-photocell-thyratron circuit had proved troublesome to adjust and keep in continuous operation, and one batch of crystals was spoiled by the relay sticking. It was therefore decided to abandon this method of temperature control and to use instead a toluene bulb with the Sunvic Proportioning Head and an electronic circuit. This had the added advantage of giving a temperature control of  $0.01^{\circ}\text{C}$  under the best operating conditions; the operating temperature could be slowly increased or decreased by hand by means of the Sunvic Proportioning Head. The circuit is described in 6.1.

The best crystals produced by this arrangement were about 5 cms. long by 1 cm. by 1 cm. and, although they contained numerous cracks and cloudy portions, yet with care in cutting and grinding, considerable portions of good, clear crystal were obtained for use in measurements. Nucleation at the surface was still troublesome and it was obvious that, if larger crystals were to be grown, hairs could no longer be used as a method of support.

A double tank of perspex was built. The inner tank, to hold the solution, was of dimensions 10" high x 12" x 12". The outer was filled with water to a level above that of the solution in the inner. The temperature of the water was controlled by the thermostat, the heaters

being situated underneath the inner tank. The floor of the inner tank was thus at a slightly higher temperature than the solution and any nuclei formed there tended to dissolve.

The inner tank was closed by a perspex sheet to exclude dust. Water vapour condensed on the relatively cold top surface and walls above the water-jacket level and streamed back into the solution, thus keeping the walls washed down. As the inner tank was practically airtight, the vapour above the solution was almost at the solution temperature, and the absence of a cold surface in contact with the solution reduced the nucleation to a minimum.

A motor mounted on top of the inner tank was geared to drive, at about 4 revs/minute, a stainless steel shaft, extending almost to the bottom of the tank. Three cross members of stainless steel were fixed to the vertical shaft at  $1\frac{1}{3}$ " intervals and, on the ends of these, the crystal seeds were mounted on small vertical rods.

The same motor drove a small propeller in the outer tank at about 100 revs/minute to keep the water in circulation.

With suitable arrangement of heaters and toluene bulb, a Beckmann thermometer test showed that the temperature swing was  $\pm 0.01^{\circ}\text{C}$ .

Crystals produced up to this point had never

exceeded 1 cm. along the a or b axes, whereas a length of 2 cms. was required along these axes. The pH of the ordinary  $\text{KH}_2\text{PO}_4$  solution is about 4.5, and, in view of the successful results obtained by adding KOH when growing nuclei, KOH was now added to the solution to bring the pH up to 6.6.

Some seed crystals grown rapidly at constant temperature by evaporation of the solution did, in fact, grow satisfactorily along the a and b axes, but when crystals were grown slowly under controlled cooling the cross-section remained the same and even showed a slight tendency to taper while growth along the c axis continued freely.

On the suggestion of Dr A.N.Holden of the Bell Telephone Laboratories, small quantities of potassium oxalate were added to the solution instead of KOH. Crystals of cross-section up to 2 cms. in the a and b directions were easily grown in a smaller bath from this solution. On account of inferior temperature control these were not of the best quality, but they were used as seeds in the more elaborate system and, from them crystals of dimensions  $2 \times 2 \times 14$  cms. were grown. The latter were mostly of very good quality while in the bath, but a few cracks were caused by siphoning out the liquid too rapidly.

The tapering of this batch was rather more pronounced and amounted to about  $2\frac{1}{2}^\circ$  towards the c axis.



For the next batch, potassium oxalate was added to the large bath to about 10 gms./litre of solution. Good crystals were grown from two good quality seeds but those grown from cracked seeds were much less satisfactory.

This time the solution was siphoned out very slowly, taking about 6 hours to siphon out 18 litres, the thermostat being left running until the process was complete. This treatment proved to be entirely satisfactory, for no cracks developed during removal from the tank, the best crystal remaining completely free from flaws.

The tapering problems had not been solved and had, in fact, increased to about  $4\frac{1}{2}^{\circ}$ . The amount of oxalate added and the general conditions of growth had not differed appreciably from that employed in the small bath when producing the original large cross-section crystals. This therefore suggested a gradual poisoning of the solution by some impurity.

It was recalled that in the large-scale production of ammonium dihydrogen phosphate, (ADP), iron is used as an inhibitor to prevent further growth along the a and b axes. The amount used is fairly critical, excess producing tapering of the crystals. For ADP about 0.06 gms./litre was found to be a satisfactory amount.

This suggested that the crystal supporting shaft of stainless steel might provide a possible source of iron, for although stainless steel tanks are used commercially for ADP without any adverse effects, KDP might be



considerably more sensitive to the presence of iron in the solution.

Accordingly, a careful examination of the quantities of iron present in the various solutions was undertaken.

The Thioglycollic acid ( $\text{HSCH}_2\text{COOH}$ ) test for iron appeared to be the most convenient and was performed as follows:- To 5 ccs. of the neutral test solution, one drop of Thioglycollic acid was added, followed by  $\frac{1}{2}$  cc. of concentrated ammonium hydroxide. The colour produced was compared with that of a standard iron solution by means of a colorimeter.

For comparison, solutions of KDP salt saturated at room temperature were used. Excess KDP was added to distilled water; the solution was heated until all was dissolved and was then allowed to cool again to give solution "A". The crystal deposit formed on the bottom was again dissolved to form a saturated solution in the same way, giving solution "B". Commercial KDP solution "A" gave .0019 gms.Fe./litre of saturated solution while solution "B" gave roughly the same. That is, recrystallisation did not appreciably change the iron content. (This figure agrees with manufacturer's estimates of the percentage of iron).

When, in the preparation of solution "A" potassium oxalate was added, the amount of iron increased to .0036 gms./litre for an oxalate concentration of about

10 gms./litre, while, for solution "B" the concentration of iron fell to much less than .001 gms./litre. (The test employed was not sufficiently sensitive to estimate less than .001 gms. Fe./litre.)

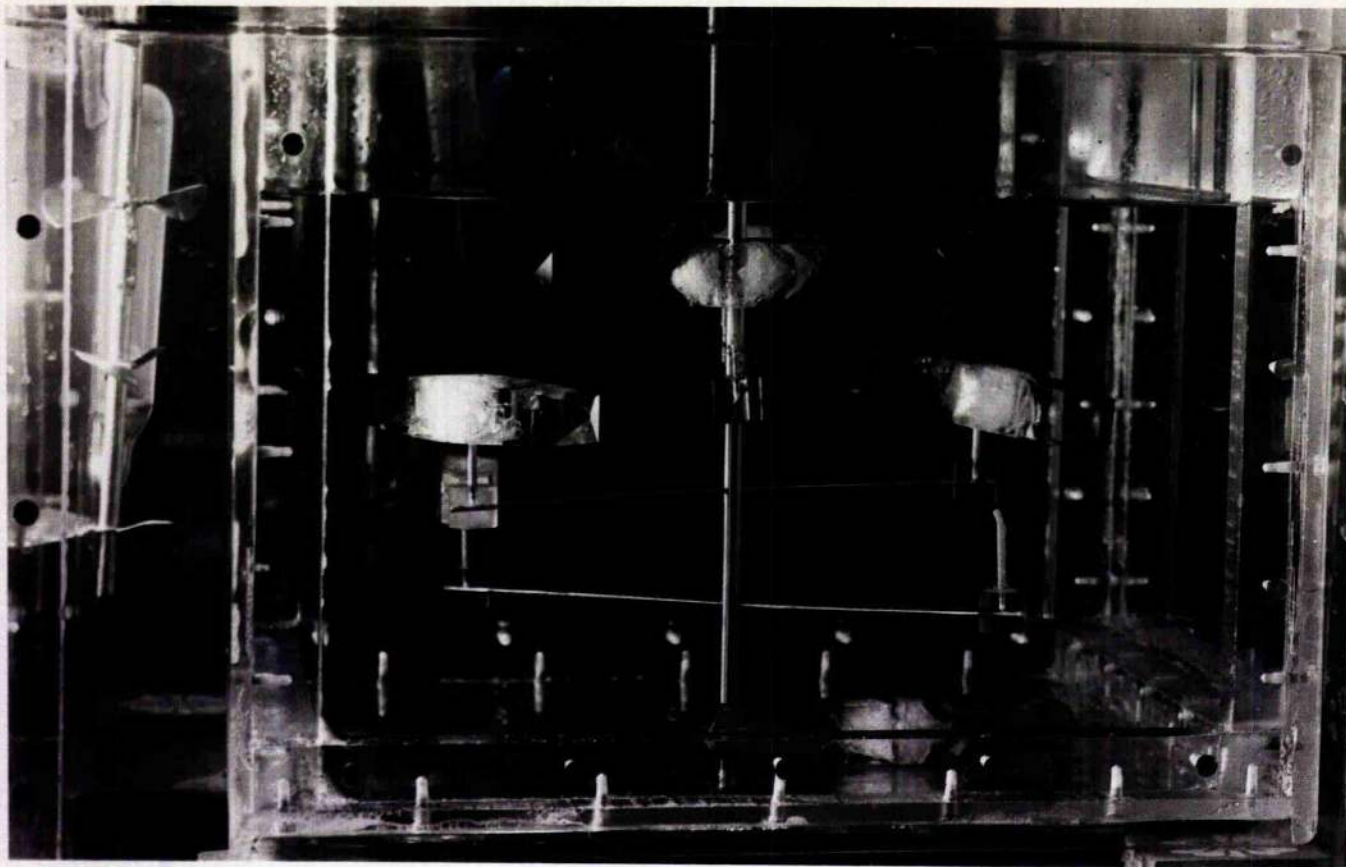
On testing the solution in the tank, it was found to contain rather more than .005 gms.Fe./litre. The iron impurity was therefore considerably greater than in an ordinary solution of the commercial salt.

An attempt was now made to purify the solution by adding oxalate to the extent of about 20 gms./litre and evaporating the solution in 6 stages until only about one litre was left. This was tested and found to contain more than .01 gms.Fe./litre and was therefore discarded. On testing the salt obtained from the six crystallizations, the iron content was found to increase gradually from less than .001 to .005 gms./litre, so the process was repeated for the last three batches.

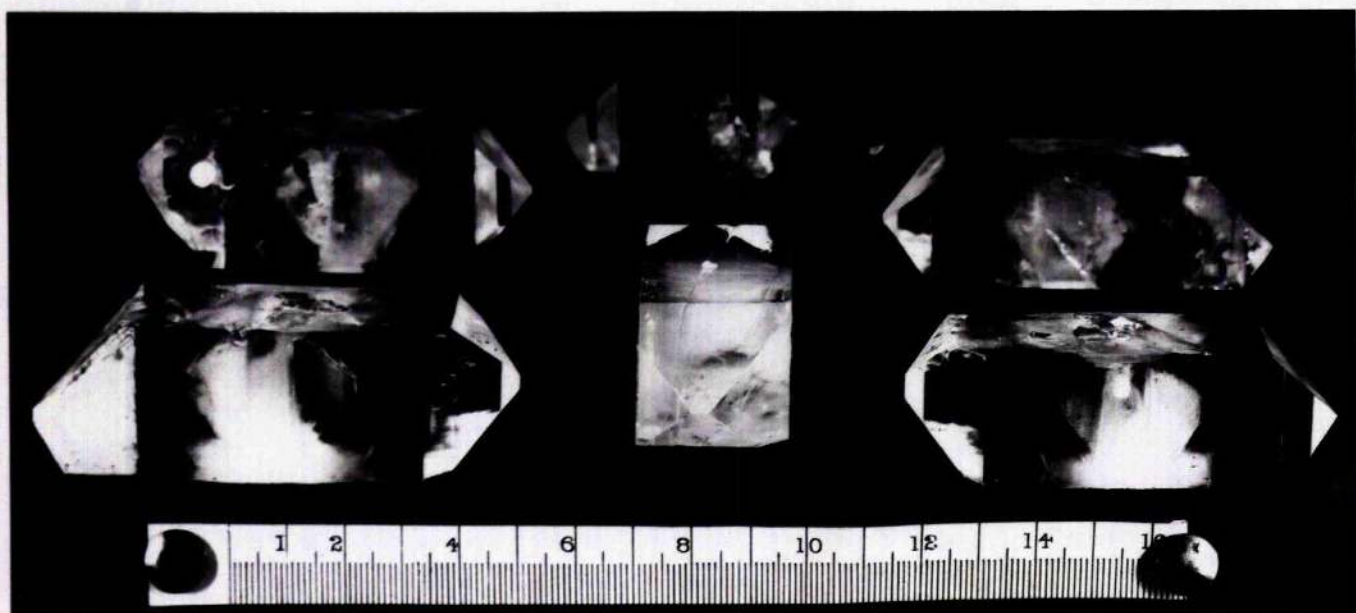
The solution was then made up again with distilled water and about 10 gms./litre of potassium oxalate were added. To avoid further contamination from the steel support, this was replaced by a glass support.

By cutting the teeth from one of the gears, the crystals were stopped for one quarter of each revolution of the main drive so that the solution and crystals did not rotate continuously together.

Starting with good seeds in the purified solution, crystals were grown showing little or no taper and were



Tapering Crystals in the Tank.



Final batch of Crystals.

removed from the tank without developing cracks. (A flaw occurring half way along their length was due to a power cut.)

A photograph of these crystals is reproduced on the opposite page (lower picture). The upper picture shows the previous batch before removal from the tank. The pronounced taper of the crystals can be seen.

## 5.2. SUMMARY OF CRYSTAL GROWING TECHNIQUE FINALLY EMPLOYED

a) Small seed crystals were produced by preparing a saturated solution of commercial KDP at  $30^{\circ}\text{C}$ . and pH concentration between 5 and 6, and allowing it to cool down rapidly. Some of the best were selected as nuclei for further growth.

b) The seed crystals were rotated in 3-4 litres of solution saturated at  $40^{\circ}\text{C}$ ., to which had been added potassium oxalate at about 10 gms./litre. The temperature of the bath was kept constant to about  $0.1^{\circ}\text{C}$ . The crystals were removed from the tank when they had reached the required length (about 2 cms.) along the a and b axes. Avoiding the central portion each was sawn into blocks of these dimensions along the a and b axes and about  $\frac{1}{4}$ " in the c direction.

In each, a hole 0.1" in diameter was drilled, parallel to the a axis, to a depth of about  $\frac{1}{2}$ ".

c) About 18 litres of solution of KDP saturated at  $50^{\circ}\text{C}$ . were prepared and carefully filtered several times. The pH concentration was adjusted to about 5 and the iron



content to .0025 gms./litre. About 10 gms. of potassium oxalate/litre were added. (With a lower iron content the oxalate would be unnecessary).

In the holes drilled in the crystal seeds, rods of stainless steel,  $\frac{3}{4}$ " long and covered with plastic, were inserted. These were attached to horizontal glass rods secured in turn to a central glass rod, the whole being supported in a perspex tank in such a way that it could be intermittently rotated by a motor. This tank was placed in a larger perspex tank, containing water, the temperature of which was controlled to  $0.01^{\circ}\text{C}$ . The outer tank was also supplied with a stirrer driven by the same motor.

After putting the crystals in position, the lid was screwed down to prevent evaporation and to exclude dust. The outer tank was filled with water to a level slightly above the estimated level of the solution; the temperature was raised gradually to the saturation temperature of  $50^{\circ}\text{C}$ . and the thermostat started.

Next, the solution was siphoned in, through a small hole in the top, at a temperature of about  $52 - 53^{\circ}\text{C}$ . to allow for cooling in transfer and to melt any small nuclei adhering to the seeds.

The crystal rotation was then started.

d) By adjusting the thermostat control, the temperature was dropped each day about  $\frac{1}{4}^{\circ}\text{C}$ .

During the first two days, pyramid ends built up

rapidly on the seed plates. A number of small pyramids appeared at first on the flat ab surfaces and these grew into each other until a complete pyramid was formed on each end. The quality of these portions was always very bad but thereafter, good, clear crystal grew along the c axis.

For a crystal about 10 cms. long, a growing period of 4-5 weeks was required, during which time the temperature dropped  $10^{\circ}\text{C}$ .

e) To remove the crystals from the tank, the rotation was stopped, but the thermostat was kept running while the solution was siphoned out very slowly to prevent cracking of the crystals by cold air being drawn in. The siphoning process required about 6 hours for 18 litres. At this speed, the air temperature above the solution remained fairly constant at about  $10^{\circ}\text{C}$ . below the bath temperature.

When all the solution had been removed, the thermostat was cut off, the water bath wrapped with felt and the whole allowed to cool down to room temperature. Thereafter, the crystals were easily removed from their supports without damage.

### 5.3. THEORIES OF CRYSTAL GROWTH.

No complete theory of crystal growth has yet been formulated, but a few points may be selected from the Faraday Society Discussion (1949).

Becker and Döring have developed a theory of



nucleation according to which fluctuations occur in the solution, beginning with two molecules, and adding a third and fourth until minute solid structures are formed. These fluctuations have an overall tendency to disperse until they reach a critical size  $r_k$  given by  $RT \log \frac{c_1}{c_{10}} = \frac{26M}{r_k \delta}$  where  $c_1, c_{10}$  are the concentrations of the supersaturated and saturated solutions respectively,  $M$  the molecular weight,  $\delta$  the density of the crystal,  $\sigma$  the interfacial free energy in contact with the supersaturated solution. Above the critical size, there is an overall tendency to grow. From the equation, the critical size is dependent on the degree of saturation of the solution.

The work of Burton and Cabrera suggests that, for growth at low supersaturation, a stepped surface is required and that, consequently, close packed surfaces will not grow because of the need for surface nucleation.

Frank has stressed the importance of spiral dislocations in supplying such a step to ensure the continuous growth of a crystal at low supersaturations.

Bunn worked on the assumption that crystals are built up in layers and that a layer, once started, is rapidly completed. He observed that the layers seemed to originate, not at the edges, but near the centre of a face, spreading out towards the edges. These layers were sometimes up to 1000A. thick and their thickness increased as they spread out from the centre. Many of his

observations were carried out with KDP, using a polarising microscope.

Buckley, in a paper on "Habit Modification in Crystals by Impurities", discredits the idea that the relative solubilities of crystal and impurity ion have any bearing on the result.

#### 5.4. OBSERVATIONS MADE DURING THE GROWTH OF KDP CRYSTALS

a) When growing small seed crystals by the process of rapidly cooling small quantities of saturated solution, it was found that an increase in the hydrogen ion concentration gave crystals with a larger ab cross-section.

The same effect could be achieved by adding small quantities of potassium oxalate; for growing large crystals the latter substance proved to be much more satisfactory.

b) On testing KDP solutions for iron (thioglycollic acid test), it was found that a saturated solution to which oxalate had been added contained a greater proportion of iron than the original solution, while crystals obtained from this solution contained less than those obtained from the untreated solution.

c) Large crystals, grown in a solution containing small quantities of iron, developed a taper of several degrees towards the c axis. Crystals could be grown without a taper from a purified solution.

d) In a solution containing more than a critical

proportion of iron, small crystals, grown slowly, tapered to a point and finally stopped growing. If the same solution was cooled rapidly, small crystals grew with little or no sign of taper.

e) On crushing and dissolving a portion of a large crystal grown in impure solution and showing a taper of  $3-6^\circ$ , practically no iron could be detected. On scraping from the tapering faces sufficient to make a small amount of saturated solution, a fairly strong iron concentration was obtained. No iron could be detected in this manner on the pyramid faces. The prism faces yielded a concentration of iron consistent with a monatomic layer of iron covering the surface.

### 5.5. DISCUSSION.

The growth mechanism observed by Bunn in microscopic KDP crystals will also apply to the prism faces of a large crystal.

We may imagine that, given adequate supersaturation, small two-dimensional nuclei will be formed at a spiral dislocation or other centre and these will spread rapidly over the crystal face. It will be possible for suitable impurities, if present, to be deposited at the growing step and so prevent the nucleus spreading over the whole surface. Further nucleation on this face will be similarly stopped and thus growth along the a and b axes inhibited. It is clear from the above observations that iron, in very small quantities, acts as an inhibitor for

the prism faces of KDP. Any agent which retains the iron in solution will decrease its effectiveness as an inhibitor. Potassium oxalate probably achieves this in our case by the formation of a complex oxalate of iron and potassium of which the solubility is sufficiently high to retain the iron in solution to a considerable extent. This would appear to indicate that the relative solubilities of crystal and impurity do play an important part.

The addition of a small quantity of iron to the solution slows down the rate of increase along the a and b axes. When a certain critical quantity of iron is present, the crystal neither grows along the a or b axes nor does it taper. Increase in the percentage of iron beyond this point causes tapering.

It was observed that spontaneous growths adhering to the crystal supports, which tapered to a point when the solution was cooled slowly, grew with scarcely any taper when the solution was cooled rapidly. This suggests that the effect of the impurity depends on the relative abundance of available solute and impurity atoms in the neighbourhood of the growing surface. Thus, in rapid cooling, when the number of solute atoms is increased while the number of impurity atoms remains constant, crystal layers are formed so rapidly that the impurity has little effect.

The deposition of iron atoms on the surface of the crystal will obey the same rules as KDP molecules, that

is, they will only readily be deposited at a step on the surface. The number of impurity atoms required to stop a growing surface is not known, but must be small. Once a surface has been stopped, then, although no further molecules of KDP can be deposited, the conditions are favourable for the further deposition of iron atoms, since a step in the surface still exists. This will continue until the whole surface has been covered by a monatomic layer of iron. It will be impossible to form a fresh nucleus of iron on account of its inadequate concentration.

By scraping a thin layer of material from a fairly large area of the tapering faces of a crystal, enough to form a few ccs. of saturated solution, the amount of iron on the surface was estimated. From the dimensions of the iron lattice for a body-centred cube, the radius of an iron atom was worked out, and from this, the number of atoms required to provide a monatomic layer for the given area was obtained. This was found to agree with the number actually found on the crystal surface within 20%.

In a solution completely free from impurities, presumably the increase along the a and b axes would equal that along the c axis.

Bunn did not observe or discuss growth on the pyramid faces of KDP; it seems unlikely, however, that nucleation occurs at the centre of these faces, but rather



the layer spreads from the edge between the pyramid and prism faces. In forming a new layer on a pyramid face, the first step must be the addition of a molecule to the *ac* or *bc* plane. If, however, the concentration of iron is such that the top *ac* plane is completely filled with iron, then a molecule of KDP cannot be added and this plane must stop growing. A KDP molecule may, however, add itself at the corner to the plane underneath and so start off a new layer on the pyramid face. The *ac* layer will continue to grow along the *c* direction, forming the starting point for further pyramid layers, until sufficient iron atoms are deposited to stop its growth. In this way, successive layers may be blocked, giving a tapering effect to the crystal.

In the nucleation process, if one or more iron atoms are deposited on a fluctuation before it reaches the critical size so that growth is hindered, the probability that it will dissolve again is increased. Hence the impurity has the effect of increasing the amount of supersaturation possible before large-scale nucleation takes place. This may be an advantage for the rapid growth of large crystals, where unwanted nucleation is often a difficulty.

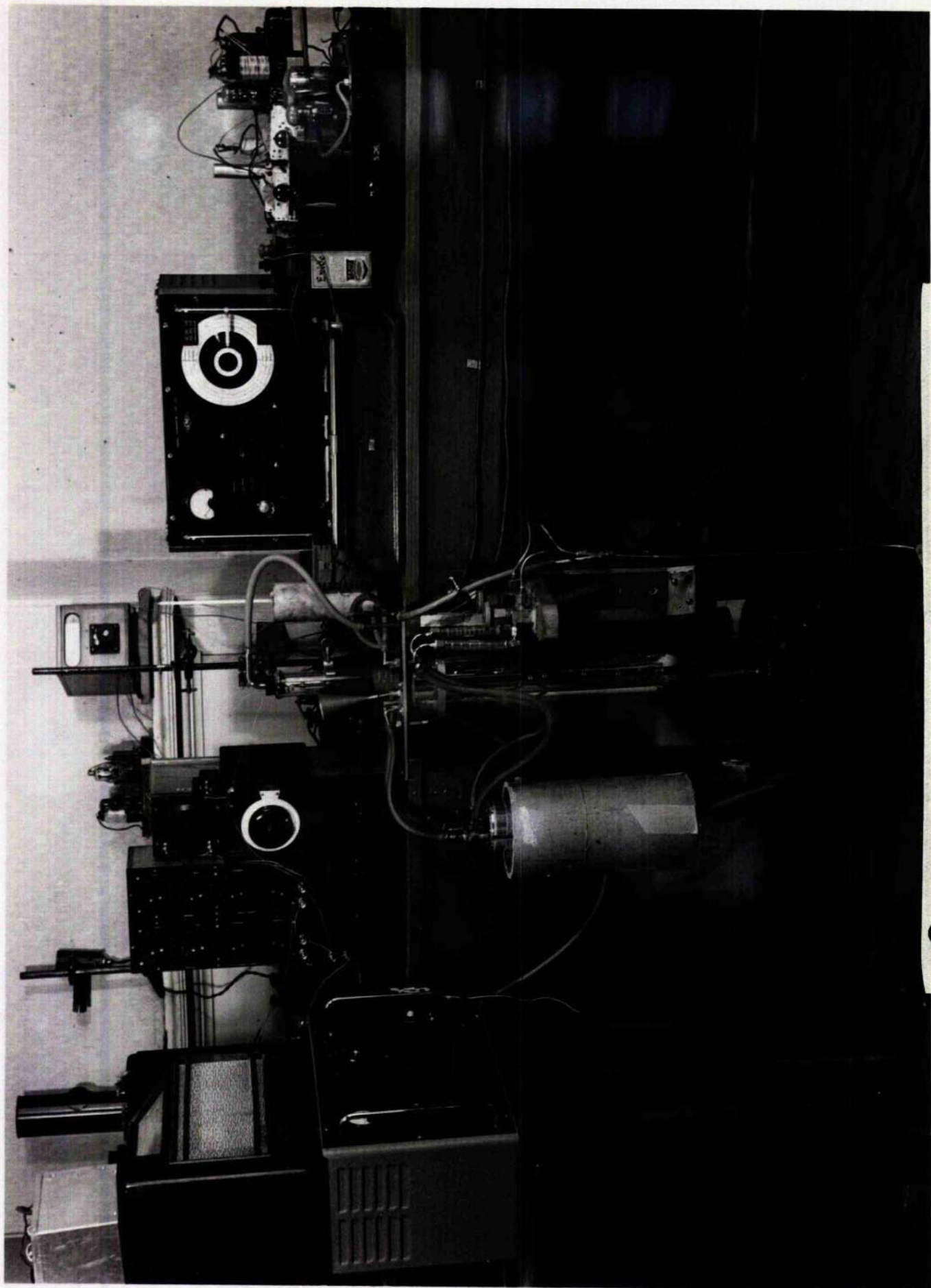
Small quantities of a suitable inhibitor present in solution may serve the dual purpose of controlling spurious nucleation and modifying the crystal habit to serve special purposes, e.g. in order to obtain crystals



of standard cross-section for sawing.

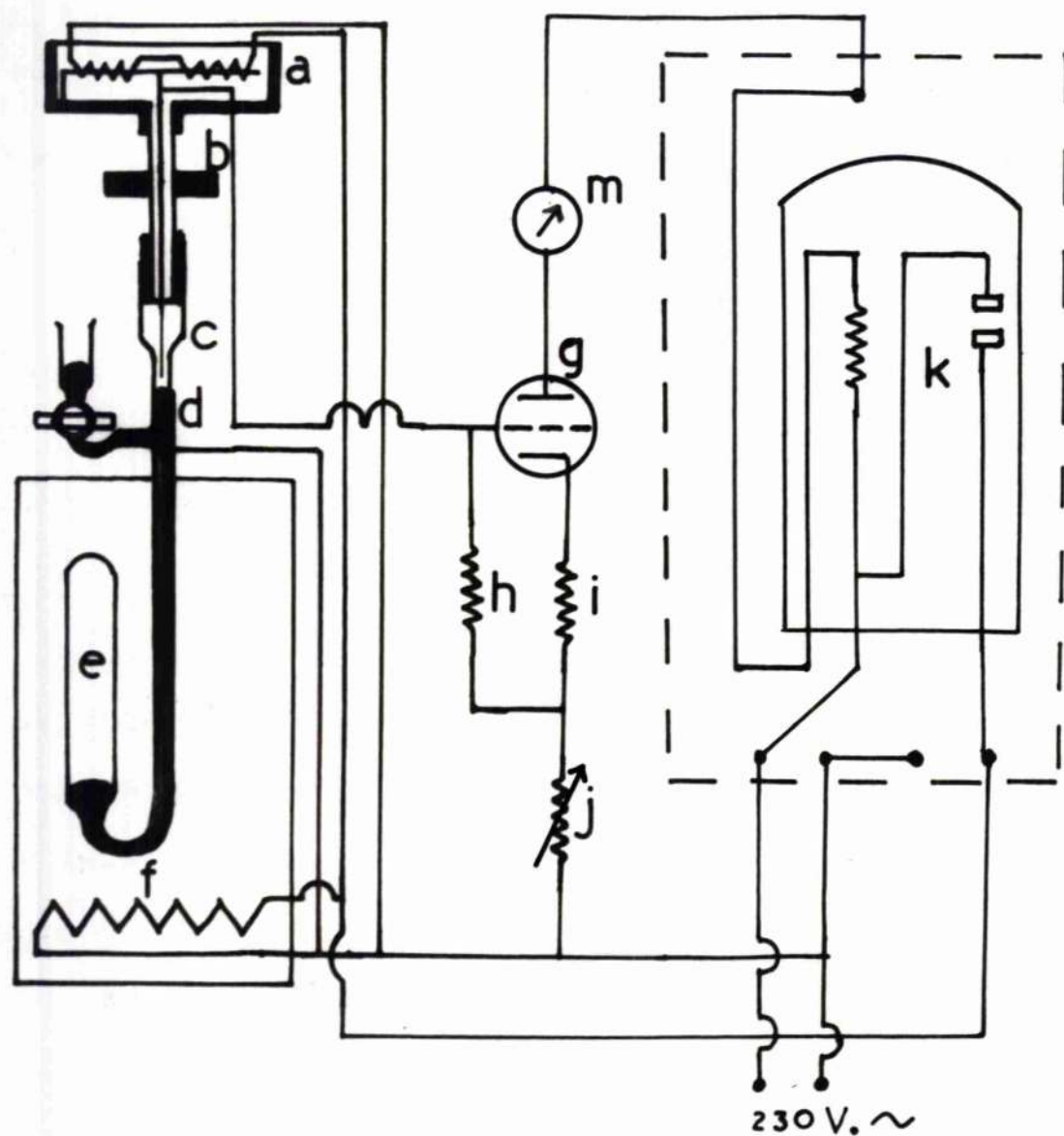
The influence of impurities and hydrogen ion concentration on the crystal form of KDP and a comparison with the behaviour of similar salts such as ammonium dihydrogen phosphate and potassium dihydrogen arsenate would merit further study. Since, however, satisfactory crystals had been obtained and since crystal growth was not the main object of the research, no further experiments were undertaken.





General View of the Apparatus.

# Temperature control circuit.



- |                     |                        |
|---------------------|------------------------|
| a—Bimetal strip.    | b—Adjusting knob.      |
| c—Adjustable needle | d—Mercury column.      |
| e—Toluene.          | f—Heater.              |
| g—6F6G.             | h— $1\text{M}\Omega$ . |
| i— $50\Omega$ .     | j— $1\text{K}\Omega$ . |
| k—Therm.vac.switch. | m—Milliammeter.        |



6.EXPERIMENTAL METHODS.6.1. TEMPERATURE CONTROL OF THE CRYSTAL TANK.

A simple toluene bulb gives temperature control of the order of  $0.1^{\circ}\text{C}$  . To get better temperature control a Sunvic Proportioning Head and thermal vacuum switch were used. A diagram is shown on page 88 .

The circuit operates as follows:-

When the needle, c, is not in contact with the mercury column, d, the valve, g, is biased by resistance, i, so that its anode current is sufficient to operate the thermal vacuum switch, k, which energises the heater, f. As the temperature rises the toluene expands and the mercury column, d, rises until contact is made with c. This earths the grid of g, the anode current drops and the switch, k, opens, cutting off the heater. With a fixed needle, c, this is equivalent to a simple toluene bulb. In the proportioning head, however, the needle, c, is suspended from a bimetal strip, a, which has its heater in parallel with the bath heater. When k is closed, the bimetal strip is heated and in expanding, lowers the needle, c, to meet the rising mercury column. When k opens, c is raised and the process repeated. Hence, superimposed on the "hunting" caused by the toluene bulb, we have a more rapid variation due to the proportioning head which smooths out the temperature variation to about  $0.01^{\circ}\text{C}$  .

The temperature of the tank can be varied from day to



day by adjusting the position of needle, c, with the adjusting knob, b. The total adjustment of the knob, b, covers about  $2^{\circ}\text{C}$ . When the end of its traverse has been reached, mercury can be let in from the reservoir to raise column d so that c can be reset again. Since the contact c - d is at the grid of the valve, very small currents are involved, and consequently, sparking at the mercury surface is minimised.

#### 6.2. CRYSTAL CUTTING AND GRINDING.

A disc of copper nickel, about 0.4 mm. thick and 3 cms. in diameter, driven by a small 12 volt motor, was mounted, with its axis horizontal, about 3 cms. above a small platform which could be moved forward by means of a screw. The crystal to be cut was mounted rigidly on this platform, lying in the appropriate direction according to the cut required, and was held in position by two clamps.

With the disc rotating rapidly, a mixture of carborundum and paraffin was fed onto the cutting edge and the platform was moved slowly forward past the disc. The rate of cutting was approximately 5 minutes per sq.cm.

Provided that the crystal was held adequately by the clamp, very little trouble was experienced from breakage.

Crystals were ground down between two glass plates, using a mixture of carborundum and paraffin, with a loop of wire as spacer between the plates. The gauge of the wire used was gradually reduced until the required



thickness was reached. Surfaces were worked to an accuracy of 1%.

Considerable care was taken to ensure that the x or z plates were cut at right angles to the crystal axes and that the bars were cut from the plates at the appropriate angles - generally  $0^\circ$ ,  $22\frac{1}{2}^\circ$ ,  $45^\circ$ ,  $67\frac{1}{2}^\circ$ . The error in angle was estimated to be less than the normal commercial limit of  $2^\circ$ . This was checked by preparing a number of crystals of the same cut and observing the variation in frequency. (3.6.2c)

### 6.3. ELECTRODES.

The electrodes for fully plated crystals were obtained by evaporating silver in vacuo.

A bell jar, about 7" in diameter, was sealed to a glass plate by a "gaco" ring, and was connected to the vacuum system by a tube through the centre of the glass plate. A stopper in the top of the bell jar carried two leads to a filament consisting of a two-stranded spiral of molybdenum 30 S.W.G wire. A number of small riders of 20 S.W.G silver wire were crimped onto this spiral which was energised by a 12v. transformer, capable of carrying 10 amps. The current was read on an avometer and controlled by a rheostat.

With a vacuum of about  $10^{-4}$  mm. of mercury in the bell jar, the current was gradually increased until the silver melted. When this was done very carefully the



small silver riders were drawn up by surface tension to form small spheres of liquid silver suspended from the molybdenum spiral. A few minutes were allowed, to burn off any impurities from the filament. The current was then switched off and the vacuum released.

Crystals to be plated were now placed on a stand inside the bell jar and the process was repeated.

A few trials determined the length of time required to give a conducting surface on the crystal face.

During the silvering of the major faces, a small amount of silver was deposited on the edge faces of the crystal, but this was easily removed by a piece of fine emery paper.

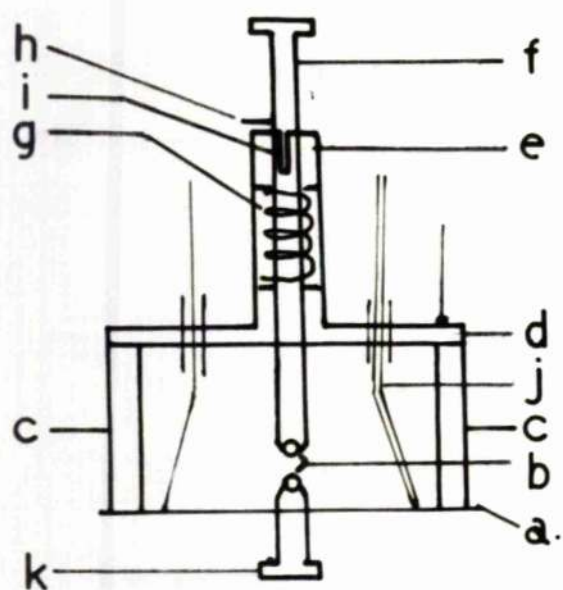
With the small central electrode (1-2 mm. in length), used for "unplated" crystals, it was found to be more convenient to cement pieces of tin foil to the crystal with "aquadag" colloidal graphite.

#### 6.4. CRYSTAL HOLDER.

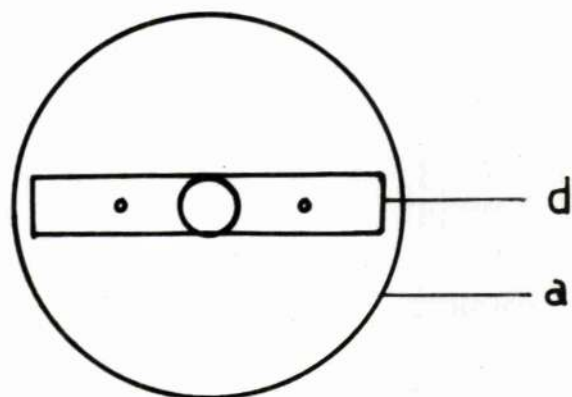
It was necessary that the crystal should be held at its nodal point, and in such a way that it remained in position while being lowered into the cryostat. It was also necessary that the heat capacity of the holder should be as low as possible. A diagram of the holder is shown on page 93 . (2 actual size)

At the centre of a brass disc, a, a small ball-

# Crystal holder.



Side Elevation.



Plan.

Twice actual size.

bearing, b, was mounted on a screw, k, so that its distance above the disc could be adjusted. Two insulating pillars, c, supported a cross bar, d, which carried at its centre a housing, e. In this was a rod, f, with a second ball-bearing, b, at its end and a weak spring, g. In the open position the projection, h, rested on top of the housing, e. When the projection, h, was brought opposite the niche, i, the spring acted so as to bring the two ball-bearings together.

Leads were taken from the bottom disc and top cross bar and a copper constantan thermocouple, j, was fastened to the bottom disc.

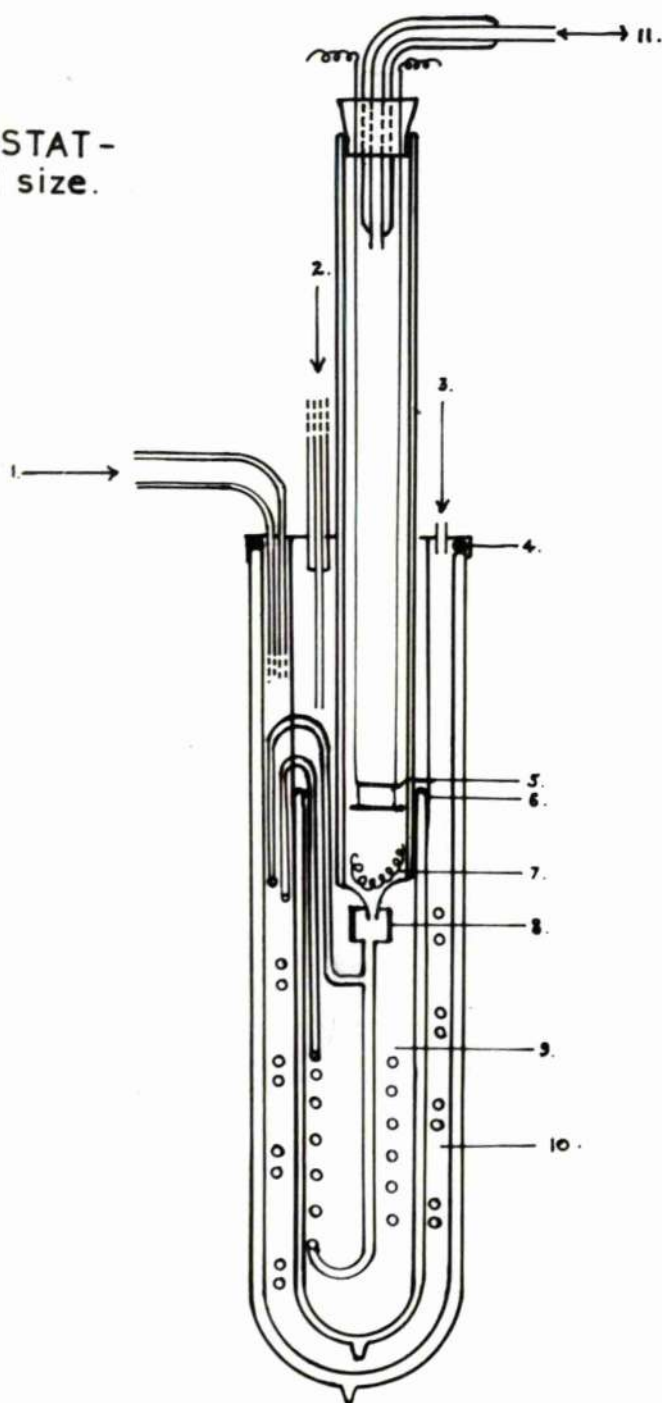
To ensure that the crystal was held at a node, it was balanced at its centre of gravity on the lower ball-bearing and the upper ball-bearing was lowered gently on top. The pressure of the spring, which could be adjusted by varying the screw, k, was sufficient to prevent the crystal slipping from its position.

Considerable care was required in construction to ensure that the common tangent to the ball-bearings was horizontal when they were brought together. (Failure to ensure this in the first model resulted in breakage of the crystal at the Curie point.)

#### 6.5. GAS CRYOSTAT.

Two streams of hydrogen gas were used to cool the crystal to the desired temperature. Both streams passed

CRYOSTAT -  
 ↓ actual size.



- 1 —  $H_2$  gas inlet.    2 — Liq.  $H_2$  filler.    3 — Liq. air filler.  
 4 — Gaco ring.    5 — Cry. holder.    6 — Rubber seal.  
 7 — Heater.    8 — Gaco ring jct.    9 — Liquid  $H_2$ .  
 10 — Liquid air.    11 —  $H_2$  exhaust.

through coils of tube immersed in liquid air. One stream was then led directly into the crystal chamber at a temperature of about  $80^{\circ}\text{K}$  while the other stream passed through a further coil, immersed in liquid hydrogen, before entering the chamber at about  $20^{\circ}\text{K}$ . By controlling the rate of flow in the two lines, any temperature, from room down to  $30^{\circ}\text{K}$ , could be obtained.

The apparatus is shown on page 95 (1/5 actual size).

The hydrogen gas flow was registered by flow meters and controlled by valves. The liquid hydrogen and liquid air containers were ordinary commercial dewars, while the measuring chamber itself was a specially prepared, long, cylindrical dewar. The connection from the metal tubing to the bottom of this glass chamber was made by a special gaco ring type of seal. To prevent freezing of the stopper and consequent leakage at the top of the chamber, the exhaust gas was led out through a small dewar tube.

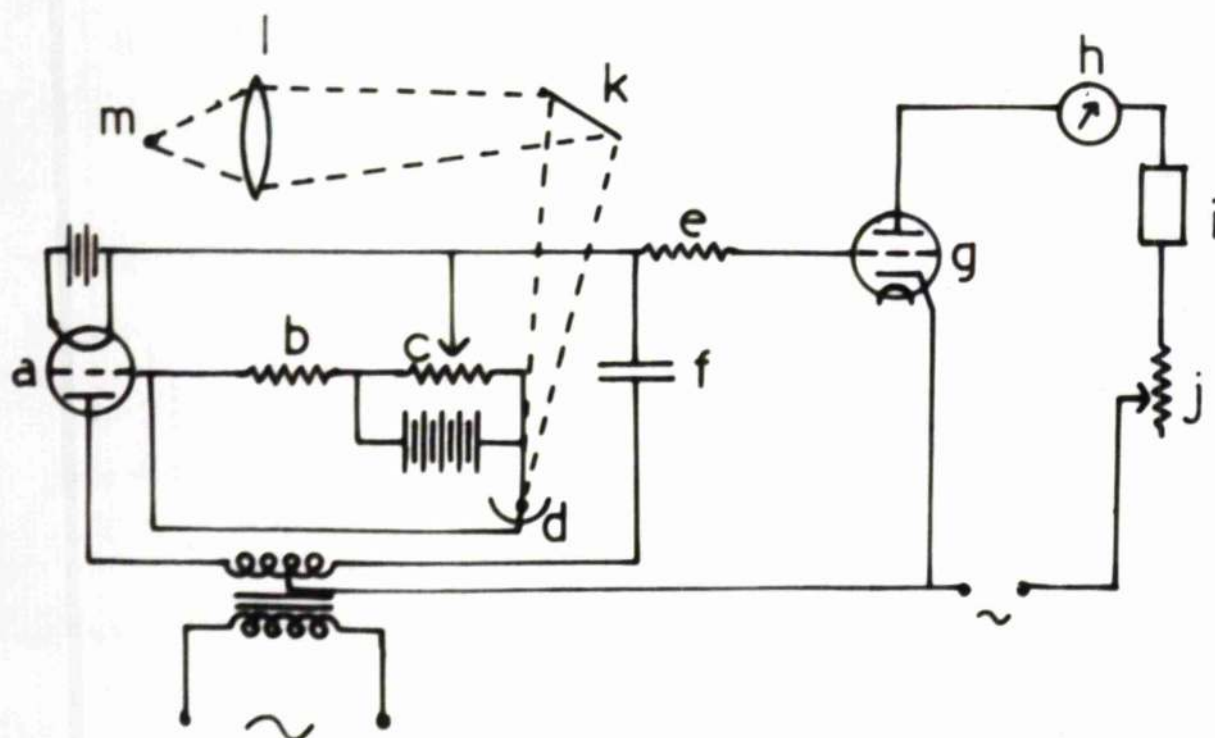
The two R.F. leads and two thermocouple leads to the crystal-holder were of fine wire (38 S.W.G.) and served to support the holder, thus cutting down heat conduction as far as possible.

#### 6.6. THERMOSTAT.

A heater and separate thermocouple for better temperature control were placed at the bottom of the inner dewar. The leads were taken up through glass capillary tubes cemented to the walls of the dewar in such a way as



## Low temperature thermostat.



a—Amplifier.

b— $1\text{M}\Omega$ .c— $500\text{K}\Omega$ .

d—Photocell.

e— $5\text{K}\Omega$ .f— $0.02\mu\text{f}$ .

g—Thyratron.

h—Milliammeter.

i— $100\Omega$  heater.j— $2\text{K}\Omega$ .

k—Galv. mirror.

l—Lens.

m—Galv. lamp.



to avoid entangling the crystal holder, and all were taken through the stopper at the top.

The thermostat circuit is shown on page 97.

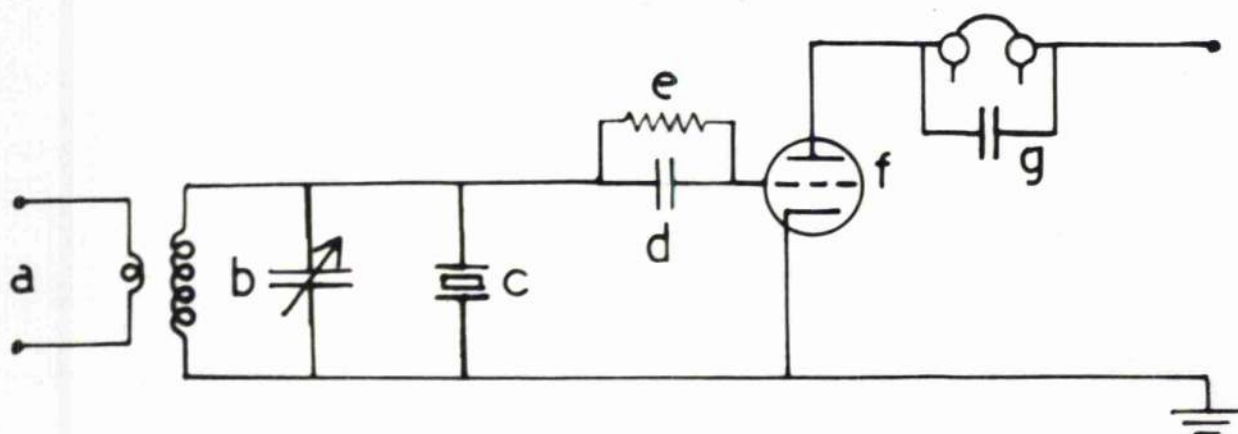
The E.M.F. of the lower thermocouple was applied to a potentiometer, the balance point of which was indicated by a galvanometer. For a particular temperature, the system was balanced so that the galvanometer lamp was focussed just off the photocell, d. The gas flow was adjusted so that the temperature in the cryostat was slowly falling. Then, as the galvanometer spot moved on to the photocell, a small current passed through the resistance, b, and increased the voltage on the grid of valve, a, so that it conducted and charged the condenser, f.

The voltage applied to the anode of the thyatron, g, was arranged to be out of phase with that applied to its grid from the transformer, so that g was biased off.

When condenser, f, charged up, this bias was removed and g conducted heavily. The heater in its anode circuit then warmed up the gas stream slightly and the galvanometer spot moved off the photocell and thus cut off the heater current.

By this means, considerably better temperature control could be achieved. (In practice, however, this device was seldom used as it was found that the temperature could be kept within  $\pm 1^\circ$  by controlling the gas flow.)

Click circuit.



a—Signal generator.

b—Resonant circuit.

c—Crystal.

d— $0.001\mu f$ .

e— $4M\Omega$ .

f—AR17.

g— $0.001\mu f$ .

### 6.7. TEMPERATURE MEASUREMENT.

To measure the temperature, a copper-constantan thermocouple was used in conjunction with a Pye potentiometer and standard cell.

A calibration curve was obtained from Landolt Bornstein and corrected for the specimen of wire used, by checking at the ice point, in liquid oxygen and liquid hydrogen.

The warm junction was kept in a mixture of ice and water in a small dewar vessel. The cold junction was hard soldered.

### 6.8. THE CLICK CIRCUIT.

This circuit (described by Cady p.385) was used to determine the approximate value of the fundamental resonance of each of the crystal specimens.

The crystal under test was placed across the tuned grid circuit of a valve, in the anode circuit of which were earphones. The frequency of a signal generator, loosely coupled to the grid circuit, was varied in jerks, beginning at low frequencies and keeping the grid circuit roughly at resonance. On passing through the natural resonance frequency of the crystal, a click was heard in the earphones.

The click is due to the fact that the crystal continues to vibrate for a short time after it has been excited and that meantime the signal generator frequency has changed. The crystal acts as a generator for this

Crystal resonance circuit.



a—Signal generator.

b—Amplifier.

c—Resonant circuit.

d—Valve voltmeter.

e—Crystal.

period and its signal beats with that of the oscillator.

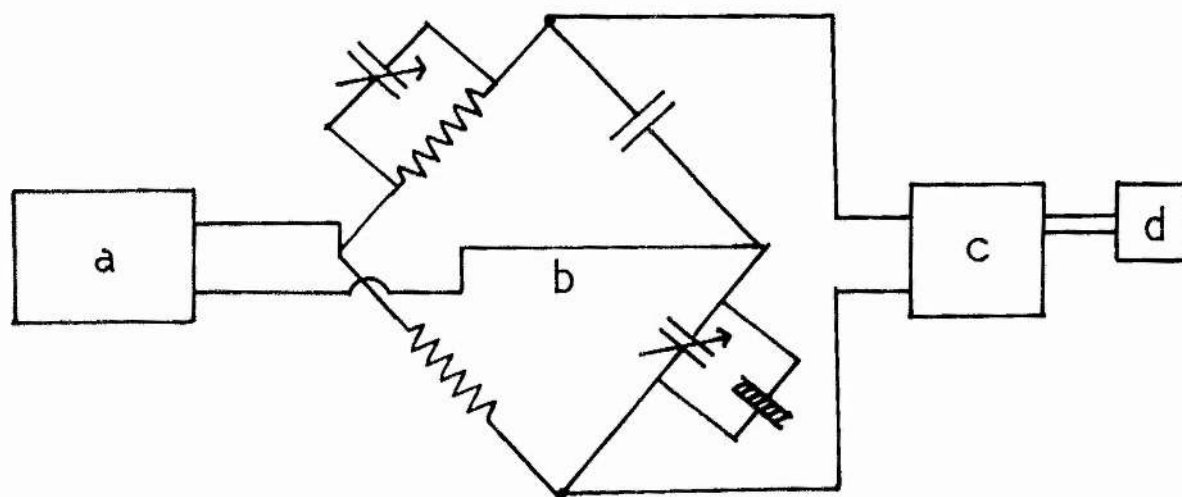
#### 6.9. MEASUREMENT OF THE RESONANT FREQUENCY.

In order to measure more accurately the resonant frequency of crystals a General Radio Company Signal Generator, type 605B, was used as a source of radio frequency. This signal generator had an additional dial which enabled frequency to be read easily to 0.1%. The output from the generator was fed through an amplifier to a resonant circuit. Across this circuit, the crystal and a valve voltmeter were placed. As the generator frequency was varied in small steps, the condenser was varied so as to keep the voltage across the crystal always at maximum. When the resonant frequency of the crystal was reached a sharp dip occurred in the valve voltmeter reading. (Dye ref.24). The bottom of the crevasse, which could be set very accurately, was taken as the resonant frequency of the crystal.

In the ferroelectric region, the crystal frequency is field dependent. Consequently, in order to measure the initial constants, it was necessary to keep the applied field small. In general, for the plated crystals in the Curie region, the voltage across the crystal did not exceed 1 volt. As the thickness of the specimens were all of the order of 1 mm., this gave a field strength of less than 10 volts per cm.



L. F. Bridge.



a—Oscillator.

b—Bridge.

c—Amplifier.

d—Speaker.

## 6.10. MEASUREMENT OF THE DIELECTRIC CONSTANT AT LOW FREQUENCIES.

To obtain the "free" dielectric constants of the crystal, the capacity of a crystal condenser was measured in a Schering Bridge at 2000 cycles. The basic circuit is shown on page 103.

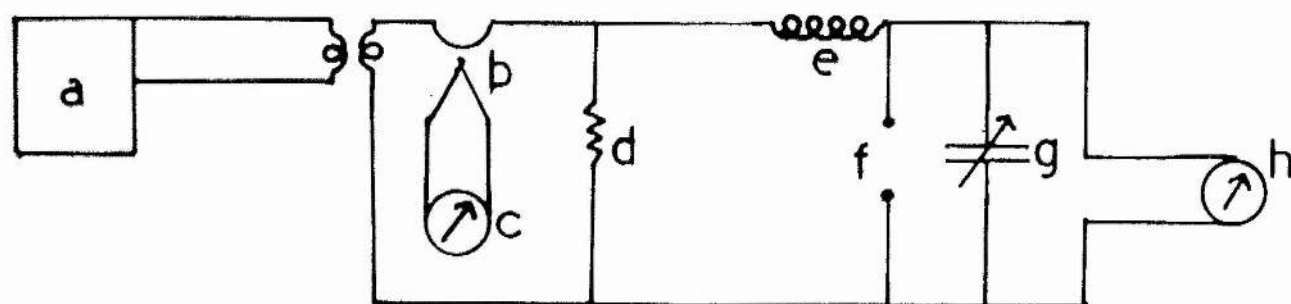
A substitution method was used in which the capacity of the crystal condenser was obtained from the change in reading of a variable condenser in parallel.

Because of the large value of the dielectric constant in the Curie region, measurements were made in three sections, 0-1000pf., 1000-10,000pf. and 10,000-100,000pf., employing different values of the bridge components in each section, to keep the bridge at its most sensitive balance.

In the 0-1000pf. range, a Muirhead standard condenser was used and this could be read to the nearest pico-farad. The overall accuracy of the apparatus was, however, probably not greater than  $\pm 2\% \pm 1$  pf. although smaller changes in capacity could be detected.

The signal was supplied by an Airmec Low Frequency generator, equipped with an attenuator. Since the total capacity in the test arm of the bridge remained the same and the bridge maintained the same balance throughout a set of readings, the voltage across the crystal was constant. In the Curie region, in order to obtain the initial free dielectric constant, the voltage was reduced

'Q' meter.



a—Oscillator.

b—Thermocouple.

c—Magn. range meter.

d— $0.04 \Omega$ .

e—Inductance.

f—Unknown capacity.

g—Calibrated ..

h—Valve voltmeter.

to give a field strength of 1 volt/cm.

### 6.11. MEASUREMENT OF THE DIELECTRIC CONSTANT AT HIGH FREQUENCIES.

In order to obtain a value approximately equal to the clamped dielectric constant, the capacity of a crystal condenser was measured at 10 Mcs by a Q meter (Marconi TFS296).

The basic circuit is shown on page 105.

A variable R.F. oscillator, a, injects a small, known, voltage into a tuned circuit consisting of e, f and g. e is an external coil and f the external condenser under test. The voltage developed across the circuit is measured by a high impedance valve voltmeter, h.

To measure the value of an external capacity, the reading of g for resonance is noted, with f terminal open circuit, and then with f connected. The difference gives the value of f.

The oscillator output can be controlled and is measured on the thermocouple meter, c. With this set to the standard mark, the valve voltmeter gives the Q of the complete circuit directly.

As the Q of the crystal condenser varies considerably in passing through the Curie point, the voltage across the condenser must also vary.

To avoid hysteresis effects in the Curie region, the capacity should be measured at constant low voltage. This was achieved by setting the Q to the lowest value

obtained near the Curie point and maintaining it at this value throughout by adjusting the oscillator output.

The voltage applied to the resistance is 20 mv., so with a Q of 40, the voltage across the crystal was .8 volts. Hence, for a condenser of thickness 1 mm, the field was 8 volts/cm.

To obtain reasonably low temperatures in the cryostat, the crystal-holder was supported by long leads of fine wire which had an appreciable resistance and inductance. This was measured and a correction applied to the condenser readings.

The estimated accuracy of measurement was  $\pm 2\% \pm 2\text{pf.}$  However, a small condenser in the instrument in parallel with g allowed changes of capacity down to 0.1pf. to be measured.



REFERENCES

- |      |                         |                           |                 |      |        |
|------|-------------------------|---------------------------|-----------------|------|--------|
| (1)  | Valasek                 | Phys. Rev.                | 17              | 475  | (1921) |
| (2)  | Busch and<br>Scherrer   | Naturwiss                 | 23              | 737  | (1935) |
| (3)  | von Hippel              | N.D.R.C. ref. no. 300     |                 |      | (1944) |
| (4)  | Mueller                 | Phys. Rev.                | 47              | 175  | (1935) |
| (5)  | Mueller                 | Phys. Rev.                | 57              | 829  | (1940) |
|      |                         |                           | 58              | 565  | (1940) |
|      |                         |                           | 58              | 805  | (1940) |
| (6)  | Beevers and<br>Hughes   | P.R.S.                    | 177             | 251  | (1941) |
| (7)  | Mason                   | Phys. Rev.                | 72              | 854  | (1947) |
| (8)  | Slater                  | J. Chem. Phys.            | 9               | 1633 | (1941) |
| (9)  | West                    | Zeits.f. Krist.           | 74              | 306  | (1930) |
| (10) | De Quervain             | Helv. Phys. Acta.         | 17              | 509  | (1944) |
| (11) | Devonshire              | Phil. Mag.                | 40              | 1040 | (1949) |
| (12) | Slater                  | Phys. Rev.                | 78              | 748  | (1950) |
| (13) | Busch                   | Helv. Phys. Acta.         | 11              | 269  | (1938) |
| (14) | Busch and<br>Ganz       | Helv. Phys. Acta.         | 15              | 501  | (1942) |
| (15) | Zwicker and<br>Scherrer | Helv. Phys. Acta.         | 17              | 346  | (1944) |
| (16) | Barkla                  | Nature                    | 158             | 340  | (1946) |
| (17) | Mason                   | Phys. Rev.                | 69              | 173  | (1946) |
| (18) | Gady                    | Piezoelectricity          | McGraw<br>Hill  |      | (1946) |
| (19) | Mason                   | Piezoelectric<br>Crystals | Van<br>Nostrand |      | (1950) |

(20)	Atanasoff and Hart	Phys. Rev.	59	85	(1941)
(21)	Mason	Phys. Rev.	50	744	(1940)
(22)	Bantle	Helv. Phys. Acta.	15	373	(1942)
(23)	Ludy	Helv. Phys. Acta	15	527	(1942)
(24)	Dye	Proc. Ph. Soc.	38	399	(1926)
(25)	Kittel	Revs. Mod. Phys	21	551	(1949)
(26)	Baumgartner	Helv. Phys. Acta	22	400	(1949)
(27)	Forsbergh	Phys. Rev.	76	1187	(1949)
(28)	Ubbelohde and Woodward	P.R.S.	188	358	(1947)

SYMBOLS.

$X$	- elastic stress
$x$	- elastic strain
$c^E$	- elastic stiffness at constant field
$c^P$	- elastic stiffness at constant polarisation
$s$	- elastic compliance
$E$	- electric field
$P$	- polarisation
$K'$	- free dielectric constant
$K''$	- clamped dielectric constant
$\eta$	- dielectric susceptibility
$\chi$	- inverse susceptibility
$d, e$	- piezoelectric constants on Voigt theory
$a, b$	- piezoelectric constants on polarisation theory
$X, Y, Z$	- coordinate axes
$X', Y', Z'$	- rotated axes
$a, b, c$	- crystallographic axes
$B$	- saturation coefficient
$\mathcal{E}$	- energy in terms of strain
$\mathcal{J}$	- energy in terms of stress
$\alpha, \beta, \gamma$	- direction cosines